GARP transcription factors repress Arabidopsis nitrogen starvation response via ROS-dependent and -independent pathways

Alaeddine Safi, Anna Medici, Wojciech Szponarski, Florence Martin, Anne Clément-Vidal, Amy Marshall-Colon, Sandrine Ruffel, Frédéric Gaymard, Hatem Rouached, Julie Leclercq, et al.

GARP transcription factors repress Arabidopsis nitrogen starvation response via ROS-dependent and -independent pathways

Alaeddine Safi (alaeddinesafi@hotmail.fr)*[1,5,6], Anna Medici (anna.medici@supagro.fr)[1], Wojciech Szponarski (szponarski@supagro.inra.fr)[1], Florence Martin (florence.martin@cirad.fr)[3,4], Anne Clément-Vidal (anne.clement-vidal@cirad.fr)[3,4], Amy Marshall-Colon (amymc@illinois.edu)[2,7], Sandrine Ruffel (sandrine.ruffel@inra.fr)[1], Frédéric Gaymard (gaymard@supagro.inra.fr)[1], Hatem Rouached (hatem.rouached@inra.fr)[1,8,9], Julie Leclercq (julie.leclercq@cirad.fr)[3,4], Gloria Coruzzi (gc2@nyu.edu)[2], Benoît Lacombe (benoit.lacombe@supagro.fr)[1], Gabriel Krouk (gkrouk@gmail.com)*[1].

(1) BPMP, Univ Montpellier, CNRS, INRA, SupAgro, Montpellier, France.

(2) New York University, Department of Biology, Center for Genomics & Systems Biology, 12 Waverly Place, New York, N.Y. 10003, USA.

(3) CIRAD, AGAP Institut, F-34398 Montpellier, France.

(4) AGAP Institut, Univ Montpellier, CIRAD, INRAE, Institut Agro, Montpellier, France.

Present Adress:

(5) Department of Plant Biotechnology and Bioinformatics, Ghent University, 9052 Ghent, Belgium.

(6) Center for Plant Systems Biology, VIB, 9052 Ghent, Belgium.

(7) Department of Plant Biology, University of Illinois at Urbana–Champaign, Urbana, IL, USA.

(8) Department of Plant, Soil, and Microbial Sciences, Michigan State University, East Lansing, MI 48824.

(9) Plant Resilience Institute, Michigan State University, East Lansing, MI 48824.

* Corresponding authors

Gabriel Krouk gkrouk@gmail.com

Alaeddine Safi alaeddinesafi@hotmail.fr

HIGHLIGHT

A nitrate-induced plant-specific transcription factor subfamily impairs the nitrate-deficiency-triggered ROS accumulation and high affinity nitrate transport. Interestingly, the quadruple mutant that we have isolated displays 2.5X more high affinity nitrate uptake activity.

ABSTRACT

Plants need to cope with strong variations of nitrogen availability in the soil. Although many molecular actors are being discovered concerning how plants perceive NO_3^- provision, it is less clear how plants recognize a lack of Nitrogen. Following N removal, plants activate their Nitrogen Starvation Response (NSR) being characterized in particular by the activation of very high-affinity nitrate transport systems (*NRT2.4*, *NRT2.5*) and other sentinel genes involved in N-remobilization such as *GDH3*. Here, we show using a combination of functional genomics via Transcription Factor (TF) perturbation and molecular physiology studies, that the TFs belonging to the HHO sub-family are important regulators of NSR through two potential mechanisms. First, HHOs directly repress the high-affinity nitrate transporters, *NRT2.4* and *NRT2.5*. *hho* mutants display increased high-affinity nitrate transport activity opening promising perspectives for biotechnological applications. Second, we show that Reactive Oxygen Species (ROS) are important to control NSR in wild type plants and that HRS1 and HHO1 over-expressors and mutants are affected in their ROS content, defining a potential feed-forward branch of the signaling pathway. Taken together our results define the relationships of two types of molecular actors controlling the NSR including: ROS and the HHO TFs. This work (i) opens perspectives on a poorly understood nutrient-related signaling pathway, and (ii) defines targets for molecular breeding of plants with enhanced NO_3^- uptake.

Keywords:

Nitrogen Starvation Response, GARP Transcription Factors, root nitrate uptake, Plant growth, cell sorting, TARGET, root protoplasts, ROS

Abbreviations:

GDH3: glutamate dehydrogenase 3

HHO : HRS1 homologue

HRS1: hypersensitive to low Pi-elicited primary root shortening 1

NSR: Nitrogen Starvation Response

NRT: Nitrate transporter

NUE: N-use efficiency

PNR: Primary Nitrate Response

PSR: Phosphate Starvation Response

ROS: Reactive Oxygen Species

TF: Transcription Factor

INTRODUCTION

Nitrogen (N) fertilization can considerably improve crop yields. Hence, it is a key requirement for global food production systems, sustaining the world's population and ensuring food security. As N is the key rate-limiting nutrient in plant growth, understanding the factors that limit N-use efficiency (NUE) will have particular relevance (Han et al., 2015). Inefficient NUE by agricultural systems is also responsible for nitrate run-off into water soil and atmosphere. Increased leaching of N into drainage water and the release of atmospheric nitrous oxide and reactive N greenhouse gases, pollute the troposphere, contribute to global warming and accelerate the eutrophication of rivers and acidify the soils (Sutton et al., 2011). Thus, understanding the regulation of N transport by plants is likely to contribute to tackle these problems.

As sessile organisms, plants need to adapt to fluctuating nutrient availability (Crawford and Glass, 1998; O'Brien et al., 2016). N related adaptations include changes in germination rate (Alboresi et al., 2005), root and shoot development (Forde and Walch-Liu, 2009; Gruber et al., 2013; Krouk et al., 2010a; O'Brien et al., 2016; Rahayu et al., 2005), flowering time (Castro Marin et al., 2010), and transcriptome and metabolome (Alvarez et al., 2020; Krouk et al., 2010a; O'Brien et al., 2016; Scheible et al., 1997; Stitt, 1999; Wang et al., 2004).

Interestingly, one can distinguish between different N-related signaling pathways being activated in response to different N variation scenarios and being reported by different sets of sentinel genes. These signaling pathways include the Primary Nitrate Response (PNR) that can be perceived when NO_3^--depleted or N-depleted plants are treated with NO_3^- (Hu et al., 2009; Medici and Krouk, 2014). PNR Sentinel genes are very rapidly regulated by NO_3^- (within minutes) (Krouk et al., 2010b) and include nitrate reductase gene 1 (*NIA1*), nitrite reductase gene1 (*NIR1*), glucose 6 phosphate dehydrogenase (*G6PDH*), and others such as the GARP (Golden2, ARR-B, Psr1) (Safi et al., 2017) transcription factors *HRS1* (hypersensitive to low Pi-elicited primary root shortening 1 (Liu et al., 2009)) and *HHO1* (HRS1 homologue 1 (Canales et al., 2014; Liu et al., 2009; Medici and Krouk, 2014)). PNR is probably the most studied and understood N-related signaling pathway for which several molecular actors have been identified. These include the NO_3^- transceptor CHL1/NRT1.1/NPF6.3 (Ho et al., 2009), number of kinases and phosphatase (CIPK8, CIPK23, ABI2, CPK10,30,32) (Ho et al., 2009; Hu et al., 2009; Leran et al., 2015; Liu et al., 2017), and several TFs (NLP6/7, TGA1, NRG2, BT1/BT2, TCP20, SPL9) (Alvarez et al., 2014; Araus et al., 2016; Castaings et al., 2009; Guan et al., 2017; Krouk et al., 2010b; Marchive et al., 2013; Wang et al., 2009; Xu et al., 2016). Recently a NO_3^--triggered Ca^{2+} signal has been shown to be a crucial relay between NRT1.1

transceptor and the nuclear events controlling PNR (Krouk, 2017; Liu et al., 2017; Riveras et al., 2015).

N-related long-distance root-shoot-root signals have also been shown to adapt plant development and metabolism to the whole nitrogen status of the plant (Gansel et al., 2001; Li et al., 2014; Ruffel et al., 2011; Ruffel et al., 2015) (Poitout et al., 2017) (Gautrat et al., 2020). These long-distance signals can be divided into N-demand and N-supply signals, which can be genetically uncoupled (Li et al., 2014; Ruffel et al., 2011; Ruffel et al., 2015). Cytokinin and CEP peptides have been shown important to generate the N-demand root-to-shoot-to-root relay necessary to regulate gene expression and modify root development in conditions where N-supply is heterogeneous (Ohkubo et al., 2017; Ruffel et al., 2011; Ruffel et al., 2015; Tabata et al., 2014) (Ota et al., 2020) (Gautrat et al., 2020).

Finally, another signaling pathway consists of N Starvation Response (NSR). It can be related to the molecular events triggered by a prolonged N-deprivation (Kiba and Krapp, 2016; Krapp et al., 2011; Menz et al., 2016). Sentinel genes of NSR include high affinity (Km ~10 µM) NO_3^- transporters *NRT2.4* and *NRT2.5* (activated to retrieve traces of NO_3^- in the soil), as well as the *glutamate dehydrogenase 3* gene (*GDH3*; hypothesized to be activated for N recycling) (Kiba et al., 2012; Lezhneva et al., 2014; Marchi et al., 2013; Yong et al., 2010). To date, NSR is still less understood than PNR at a molecular level. The calcineurin B-like7 calcium sensor displayed an effect on *NRT2.4* and *NRT2.5* expression in the context of NSR (Ma et al., 2015). A role of miR169 was shown in the control of NFYA TFs in response to NSR with a substantial impact on *NRT2.1* and *NRT1.1* transcriptional regulation (Zhao et al., 2011). However, no proof of the actual role of *NFYA* genes themselves on NSR was provided in this work work (Zhao et al., 2011). LBD37,38,39 TF over-expression has been shown to impact anthocyanin production in N-deprived plants with a potential regulation of nitrate transporters including *NRT2.5* (Rubin et al., 2009). However, no direct regulatory targets of LBDs were provided (Rubin et al., 2009). Finally, recent reports showed that HRS1/HHOs (aka NIGTs) are transcriptional regulators of *NRT2.4* and *NRT2.5* (Kiba et al., 2018; Maeda et al., 2018).

Reactive Oxygen Species (ROS) are produced during normal cell metabolism and are now largely accepted to be key signaling molecules (Choudhury et al., 2017). Their roles range from physiological to developmental processes such as: biotic and abiotic stress response, cell division, cell elongation and programmed cell death (Foyer and Noctor, 2013; Noctor et al., 2018). In the context of nutritional signaling pathways, ROS are known to be produced upon N, P and K starvation (Jung et al., 2018; Shin et al., 2005; Shin and Schachtman, 2004). Altering ROS production indeed affects

transcriptional responses to K deficiency (Shin and Schachtman, 2004). But for N, evidence of ROS as potential second messengers is still scant.

Recently CC-type glutaredoxins were shown to be highly N-responsive and their over-expression modifies *NRT2.1* responsiveness to nitrogen (Jung et al., 2018). Also very recently, *HNI9* which is potentially involved in N response (Widiez et al., 2011), was shown to display ROS accumulation that correlates with *NRT2.1* transcriptional control (Bellegarde et al., 2019). Despite these interesting indirect evidences, the role of ROS *per se* in NSR has never been directly demonstrated.

Here, we show that NO_3^- regulation of one of the most strongly and rapidly induced TF (HRS1) (Canales et al., 2014; Krouk et al., 2010b) and its close homologs (HHOs) (Safi et al., 2017), , are involved in NSR regulation through likely two parallel mechanisms. First, HHOs being PNR responsive are repressors of NSR *via* direct repression of *NRT2.4, NRT2.5, GDH3* genes. This regulation, when abolished in a quadruple *hho* mutant, dramatically increases NO_3^- HATS, leading to striking phenotypes with potential biotechnological applications. This provides new insight into the molecular connection between PNR and NSR signaling. Second, ROS scavenging treatments concomitant to N deprivation treatments totally abolishes NSR showing that ROS accumulation is a prerequisite to NSR. Third, *HHO* genetic manipulations (over-expression and KO mutations) impair ROS accumulation and/or metabolism of the plants. These observations brought us to build a working model in which the HHOs control two parallel branches of NSR response in Arabidopsis including one that involves ROS.

MATERIAL AND METHODS

Plant material. All Arabidopsis (*Arabidopsis thaliana*) plants were in the Columbia-0 background. *hrs1-1* (SALK_067074), *hho1-1* (SAIL_28_D03) (Medici et al., 2015) *hho2-1* (SALK_070096) and *hho3-1* (SALK_146833) mutants were obtained from ABRC seed stock center and homozygous lines were screened by PCR. The double (*hrs1;hho1*), triple (*hrs1;hho1;hho2*) and quadruple (*hrs1;hho1;hho2;hho3*) mutants have been obtained by crossing. The *promoter:gene:GFP* lines were obtained by cloning 3-kb upstream promoter region followed by *HRS1* gene (genomic sequence) into pMDC107 Gateway-compatible vector (Curtis and Grossniklaus, 2003).

The over-expressor lines were obtained by cloning HRS1- and HHO1-coding sequences into pMDC32 Gateway-compatible vector (Medici et al., 2015). The constructs were transferred to GV3101 *Agrobacterium tumefaciens* strain and used in plant transformation by floral dip (Zhang et al., 2006).

Growth conditions and treatments. Plants were grown in sterile hydroponic conditions for 14 days in day/night cycles (16/8 h; 90 µmol photons m^{-2} s^{-1}) at 22°C as described in Krouk et al. (2010b). The hydroponic medium consisted of 1 mM KH_2PO_4, 1.5 mM $MgSO_4$, 0.25 mM K_2SO_4, 3 mM $CaCl_2$, 0.1 mM Na-Fe-EDTA, 30 µM H_3BO_3, 5 µM $MnSO_4$, 1 µM $ZnSO_4$, 1 µM $CuSO_4$, 0.1 µM $(NH_4)_6Mo_7O_{24}$, 5 µM KI; supplied with 3 mM sucrose, 0.5 mM NH_4NO_3 (1 mM KNO_3 for results in figure 1) and 0.5 g L^{-1} MES. pH was adjusted to 5.7 by adding KOH 1M. For +N → -N experiments, plants were transferred to an equivalent fresh N-free or 0.5 mM NH_4NO_3-containing medium (1 mM KNO_3 for results in figure 1). For -N → +N experiments, all plants have been N-starved for 3 days, and then transferred to an equivalent fresh medium containing 0.5 mM NH_4NO_3. ROS-scavenging drugs were applied upon plant transfer to the new medium. Roots (corresponding to approximately 60 plants coming from a single phytatray) were harvested at different time points and immediately frozen in liquid nitrogen. Each time point and genotype being harvested from a different phytatray. Experiments have been performed at least twice and representative data are reported in figures.

For non-sterile hydroponic culture, seeds were sown on Eppendorf tube caps with 1 mm whole filled by H_2O-agar 0.5% solution and grown for 7 days on H_2O. Then, plants were transferred to the same medium as above (without sucrose) and supplied with 0.5 mM NH_4NO_3 and grown in short day light period (8h light 23°C and 16h dark 21°C) at 260 µmol photons $m^{-2}.s^{-1}$ and 70% humidity. The nutritive solution was renewed every 4 days for 5 weeks. Then plants were transferred to an equivalent fresh N-free or 0.5 mM NH_4NO_3-containing medium (1 to 3 weeks for $^{15}NO_3^-$ uptake experiments and 6h for ROS measurements).

For mutant complementation experiments (Fig. 2D), wild type and complemented (*hrs1;hho1;hho2;hho3;pHRS1:HRS1:GFP*) sterilized seeds were sown on the surface of sterile solid N-free MS/2 basal salt medium (1% (w/v) agar), supplemented with 3 mM sucrose, 0.5 mM NH_4NO_3 and MES-buffered at pH 5.7 (0.5 g L^{-1}). Agar plates were incubated vertically in an *in vitro* growth chamber for 12 days in day/night cycles (16/8 h; 90 µmol photons $m^{-2}.s^{-1}$) at 22 °C.

Real-time qPCR analysis. Total RNA was extracted from Arabidopsis roots using Trizol® (Thermo Scientific) and digested with DNAseI (Sigma-Aldrich). RNA was then reverse transcribed to one-strand complementary DNA using Thermo script RT (Invitrogen) according to the manufacturer's protocol. Gene expression was determined by quantitative PCR (LightCycler 480; Roche Diagnostics) using gene-specific primers (provided upon request) and TAKARA mix (Roche). Expression levels of tested genes were normalized to expression levels of the *Actin* and *Clathrin* genes as previously described (Krouk et al., 2010b).

Expression and purification of GST-HRS1 protein. The protocol is fully described in (Medici et al., 2015). Briefly, *HRS1* coding sequence was first inserted in pDONR207 vector, and then transferred to pDEST15 vector (Invitrogen) following the manufacturer's instructions. GST-HRS1 fusion protein was expressed in *Escherichia coli* Rosetta 2(DE3)pLysS (Novagen). Transformed bacteria were grown in Terrific broth medium at 37°C containing the appropriate antibiotics until the OD660 reached 0.7-0.8. After induction with 1 mM IPTG for 16 h at 22° C, cells were harvested by centrifugation (6000 g, 10 min, 4°C) and suspended in 1X PBS buffer containing lysozyme from chicken egg white (Sigma) and complete protease inhibitor cocktail (Roche). The resulting cell suspension was sonicated and centrifuged at 15000 g, for 15 min at 4°C to remove intact cells and debris. The protein extract was mixed with buffered glutathione sepharose beads (GE Healthcare), and incubated at 4°C for 3 h. The resin was centrifuged (500 g, 10 min, 4°C) and washed five times with 1X PBS buffer.

GST-HRS1 was then eluted with 10 mM reduced glutathione (Sigma) in 50 mM Tris buffer and dialyzed overnight in 150 mM NaCl, 50 mM HEPES, pH 7.4 buffer.

All fractions were subjected to SDS-PAGE. For protein quantification, absorbance was measured on a VICTOR2™ microplate reader (Perkin Elmer) at 660 nm using the Pierce 660 nm Protein Assay (Pierce/Thermo Scientific).

Electrophoretic Mobility Shift Assay. EMSA was performed using purified GST-HRS1 protein and 3' end Biotin_TEG-labeled DNA probes. Single-stranded DNA oligonucleotides were incubated at 95 °C for 10 min and then annealed to generate double-stranded DNA probes by slow cooling. The sequences of the oligonucleotide probes were synthesized by Eurofins Genomics and are provided in Supplementary Fig. S6. The binding of the purified proteins (~ 150 ng) to the Biotin_TEG-labeled probes (20 fmol) was carried out using the LightShift Chemiluminescent EMSA Kit (Thermo Scientific)

in 20 µL reaction mixture containing 1X binding buffer (10 mM Tris, 50 mM KCl, 1 mM DTT, pH 7.5), 2.5% glycerol, 5 mM $MgCl_2$, 2 µg of poly (dI-dC) and 0.05 % NP-40. After 30 min of incubation at 24° C, the protein–probe mixture was separated in a 4% polyacrylamide native gel at 100 V for 50 min then transferred overnight to a Biodyne B Nylon membrane (Thermo Scientific) by capillarity in 20X SSC buffer. After ultraviolet crosslinking (254 nm) for 90 s at 120 $mJ.cm^{-2}$, the migration of the Biotin_TEG-labeled probes was detected using horseradish peroxidase-conjugated streptavidin in the LightShift Chemiluminescent EMSA Kit (Thermo Scientific) according to the manufacturer's protocol, and then exposed to X-ray film.

ROS measurement. An Amplex® Red Hydrogen Peroxide/Peroxidase Assay Kit (Molecular probes) was used to measure H_2O_2 production in 6-week-old plants, according to the manufacturer's protocol. Six independent roots for each treatment and genotype were frozen and ground in liquid N. All the protocol steps were carried out in a cold room at 4 °C. Two hundred microliters of phosphate buffer (50 mM K_2HPO_4, pH 7.4) was added to 50 mg of ground frozen tissue. After 2 centrifugations at 14000 g for 10 min, 50 µl of the supernatant were added to 50 µl of the Amplex® Red mixture (100 µM 10-acetyl-3,7-dihydroxyphenoxazine and 0.2 U/ml horseradish peroxidase) and incubated in the dark at room temperature for 30 min. The absorbance was measured using VICTOR2™ microplate reader (Perkin Elmer) at 560 nm in 96-well transparent plates. A blank (containing 50 µL phosphate buffer and 50 µL Amplex® Red reagent) was used as a negative control. H_2O_2 concentration was reported to the exact powder mass of each sample. The absorbance was measured twice for each point.

Nitroblue Tetrazolium (Sigma-Aldrich) was used for superoxide ($O_2^{\bullet -}$) staining. Plants were vertically grown on 0.5 mM NH_4NO_3-containing medium for 2 weeks. Whole freshly-harvested plants were stained for 15 min in 20 mM phosphate buffer pH 6.1 containing 2 mM NBT. The seedlings were subsequently washed using the same buffer.

Antioxidant enzyme (APX, GR, GPX) activity measurements were performed as previously described (Leclercq et al., 2012).

$^{15}NO_3^-$ uptake. Root $^{15}NO_3^-$ influx was assayed as previously described (Lejay et al., 1999). Plants were sequentially transferred to 0.1 mM $CaSO_4$ for 1 min and then to basal nutrient medium (pH 5.7) containing appropriate concentrations of $K^{15}NO_3$. In the labeling solution, $K^{15}NO_3$ was used at 10 to 250 µM for HATS and at 1 to 5 mM for LATS. After 5 min, roots were washed for 1 min in 0.1 mM $CaSO_4$, harvested, dried at 70°C for 48 h and analyzed. The total N content and atomic percentage ^{15}N abundance of the samples were determined by continuous-flow mass spectrometry as previously described (Clarkson et al., 1996), using a Euro-EA Eurovector elemental analyzer coupled with an IsoPrime mass spectrometer (GV Instruments). Each uptake value is the mean +/- SE of 6 replicates (6 independent roots from different plants).

Phylogenetic analysis. The phylogeny reconstruction was established as described in (Safi et al., 2017) on the whole protein sequences. Briefly, the tree was built using the mafft algorithm (http://mafft.cbrc.jp/alignment/server/, parameters: G-INS-1, BLOSUM62) and drawn with FigTree. Different parameters including FFT-NS-2, FFT-NS-i, E-INS-i were used and they yielded very similar trees.

TF perturbation assays in the TARGET system. The TARGET procedure was performed as previously described (Bargmann et al., 2013; Medici et al., 2015). Root protoplasts were treated with 35 µM CHX (Cycloheximide) for 30 min, then 10 µM DEX (Dexamethasone) were added and cell suspension was incubated in the dark overnight at room temperature. Controls were respectively treated with DMSO and ethanol.

The red fluorescent protein was used as a selection marker for fluorescent-activated cell sorting of successfully-transformed protoplasts. N-free buffers were maintained during the whole procedure (as compared to Medici et al. (2015) where NO_3^- was maintained during the TARGET procedure). RNA was extracted and amplified for hybridization with ATH1 Affymetrix chips.

Transcriptomic analysis was performed using ANOVA followed by a Tukey test using R (https://www.r-project.org/) custom made scripts following previously published procedures (Obertello et al., 2010; Ristova et al., 2016). Clustering was performed using the MeV software (http://mev.tm4.org/). Briefly, the ANOVA analysis was carried out using the R *aov()* function on log2 MAS5-normalized data. A probe signal has been modeled as follows: $Yi = \alpha_1.DEX + \alpha_2.NO3 +$

α_3.NO3*DEX + ε; where α1 to α3 represent the coefficient quantifying the effect of each factor (DEX, NO_3^-) and their interaction (DEX*NO_3^-), and ε represents the unexplained variance. We determined the false discovery rate (FDR) to be <10% for an ANOVA p value-cutoff of 0.01 and a Tukey p value-cutoff of 0.01.

Statistical Analysis

Mean +/- SE is shown for all numerical values. Statistical significance was computed using a two-tailed Student's t test. Significance cutoff: * P < 0.05, ** P < 0.01, *** P < 0.001.

ANOVA and Tukey tests for TARGET and ROS signature clustering are described in Materials and Methods and fully detailed protocols are provided upon request.

RESULTS

During our previous investigations, we studied the role of HRS1 in the control of the primary root growth in response to a combination of N and P provision (Medici et al., 2015). This research led to the identification of a set of HRS1 direct targets. In that study, we noted that *NRT2.4* transcript accumulation was repressed upon controlled nuclear entrance of the GR:HRS1 fusion protein (Supplementary Fig. S1A at JXB online) (Bargmann et al., 2013; Medici et al., 2015). We also observed that *NRT2.4* was over-expressed in the double *hrs1;hho1* mutant (Fig. S1B). These preliminary results suggested that HRS1 could be a direct regulator (e.g. repressor) of *NRT2.4* gene. Moreover, as *NRT2.4* was shown to be a very good marker of NSR (Kiba et al., 2012), and no regulator was shown to participate in this signaling pathway at the outset of our study, we decided to investigate the role of HRS1 and its close HHO homologs in the NSR response. Since the experiments on the HRS1/HHO family in Medici et al. (2015) (Fig. S1B) were performed on plants grown in very particular conditions (low Phosphate, high N), in this current study we investigated the behavior of the *hrs1;hho1* mutants and HRS1, HHO1 over-expressors (Fig. S1A) in the specific context of the NSR (transfer of plants from N containing media to N-free media). To consolidate our investigations, we also studied two other genes considered as NSR sentinels, namely *NRT2.5* (Lezhneva et al., 2014) and *GDH3* (Marchi et al., 2013).

HHO transcription factors repress NSR sentinel genes

Consistent with previous findings (Kiba et al., 2012), when transfered to N-depleted medium, WT plants show strong activation of *NRT2.4*, *NRT2.5* and *GDH3* genes within the first days of starvation (Fig. 1A). This response defined as NSR is diminished in 35S:HRS1 plants though. NSR marker genes are also affected in the *hrs1;hho1* double mutant as they peak earlier and are also repressed at earlier time-points compared to WT (Fig. 1A). Given that HRS1 and HHO1 are homologous genes, and because the double mutant has a NSR phenotype, we set up an experiment to compare HRS1 and HHO1 over-expressors side-by-side. This experiment (Fig. 1B) showed that indeed 35S:HRS1 and 35S:HHO1 display similar molecular phenotypes with a reduction of the NSR response. Taken together, these results suggest that HRS1 and HHO1 are repressors of NSR, likely through the direct regulation of *NRT2.4* and *NRT2.5* loci.

One interesting aspect of the *hrs1;hho1* double mutant, was a very variable response across experiments to NSR with the most representative response shown in Fig. 1A. This can be explained by the previous findings that showed that HRS1, HHO1 and its paralogs HHO2 and HHO3 are all transcriptionally regulated by PNR (Krouk et al., 2010b; Wang et al., 2004). To understand the interactions of the HHO paralogs in regulating the NSR, we generated plants with an increasing number of deletions in this gene sub-family (Fig. 2A). We created the triple *hrs1;hho1;hho2* and quadruple *hrs1;hho1;hho2;hho3* mutants by crossing (characterization in Fig. S2B) and compared them with WT, single and double mutants. The rationale was that if these HRS1/HHO TFs are indeed repressors of NSR, they could strongly be regulated by nitrate (in the context of the PNR) in order to rapidly stop the NSR response when NO_3^- is available. We thus tested this hypothesis by subjecting the plants (WT, single, double, triple and quadruple *hrs1/hho* mutants) to a nitrogen starvation treatment first, then treated them with NO_3^-, and then followed the speed of NSR sentinel gene repression (Fig. 2B). In this context, we showed that in WT, consistent to what was observed by Okamoto et al. (2003), NSR sentinels peak within minutes and are strongly repressed within 2 to 4 hours following NO_3^- provision (Fig. 2B). As predicted, the sequential deletion of the *HHO* paralogs triggers a de-repression of NSR genes. It is noteworthy that the de-repression of the NSR sentinel genes follows the sequential deletion of *HHOs* (quite manifest at the 2 and 3 hour time-points) (Fig. 2C). HRS1/HHO quadruple mutant displays the strongest phenotype and seems to be unable to completely repress the locus even after several hours of NO_3^- provision (Figs. 2B, 2C).

To validate that it is indeed a combination of *HRS1/HHO* deletion that de-repressed the NSR sentinels (as opposed, for example, to the simple effect of *hho3* mutation), we performed a complementation experiment of the quadruple *hrs1;hho1;hho2;hho3* mutant with pHRS1:HRS1:GFP.

We showed (Fig. 2D) that two independent lines are able to fully restore the WT phenotype regarding the NSR sentinel gene expression. This demonstrates that it is indeed a combination of *HRS1/HHO* deletions that is needed to observe the de-repression of NSR genes (Figs 2B-2D).

These results show that HHOs have a redundant function and that they collectively are involved in repressing NSR sentinels when NO_3^- is provided (Fig. 2).

HHO transcription factors control NO_3^- uptake via HATS

Among the three NSR sentinel genes, *NRT2.4* and *NRT2.5* were shown to be involved in a very high-affinity nitrate transport system (Kiba et al., 2012; Lezhneva et al., 2014). Since we observed interesting molecular phenotypes in the context of N-starvation for the 35S:HRS1 and *hrs1;hho1* mutants (Fig. 1), we tested their high-affinity transport system (HATS) activity following prolonged NO_3^- starvation (Fig. 3A). We performed $^{15}NO_3^-$ labeling experiments, and indeed found that 35S:HRS1 plants are affected in NO_3^- HATS (10 µM) activity. We subsequently seeked to determine the range of affinities at which HRS1 over-expression may have an effect. We observed (Fig. 3B) that the whole high-affinity range was decreased in the 35S:HRS1 plants (with a 2-fold decrease for the very high nitrate affinity conditions, concomitant with a decrease in *NRT2.4*, *NRT2.5*, *NRT2.1* mRNA accumulation), while low affinity nitrate transport activity remained unchanged in the 35S:HRS1 background (Fig. 3B). The double mutant *hrs1;hho1* displayed a weak phenotype in this context, as compared to the WT.

Since we showed that the *hrs1/hho* mutants were unable to totally repress the *NRT2.4*, *NRT2.5* loci (Fig. 2B), we also wanted to study functional phenotypes in these mutants. Thus, we performed $^{15}NO_3^-$ labeling experiments on N-containing media (Fig. 4A). Consistent with our previous findings (Fig. 2B), the sequential deletion of *HHOs* (Fig. 2A) increases NO_3^- HATS activity with a maximum effect recorded in the *hrs1;hho1;hho2;hho3* quadruple mutant that displays a 2.5 fold increase of HATS activity (Fig. 4A). Very interestingly, the nitrate transport activity increase is accompanied with a strong stimulation of the quadruple mutant growth in these conditions (Fig. 4B). Although its phenotype is less pronounced than in the quadruple mutant, the double mutant *hrs1;hho1* still displays larger shoots as compared to the wild type (Fig. S3). The mutant phenotypes were lost in plants grown on –N conditions. This can be easily explained. Indeed, even if *NRT2.4* and *NRT2.5* are de-repressed in the mutants in both conditions, only the mutants grown on +N can take up more nitrate than WT. Furthermore, HHOs expression is known to be very low in –N conditions (Krouk et al., 2010b; Menz et al., 2016), so mutations of genes, being weakly expressed in -N, are

expected to have low or no effect. These are two possible explanations of why we see mutant phenotypes only on +N conditions. Furthermore, the quadruple mutant displays strong phenotypes following N provision even for genes not previously known to be involved in NSR such as *NRT1.1, NRT2.2* or *NAR2.1* (Fig. S4). However a very recent study reported that heterologous expression of *DsNAR2.1* (*Dianthus spiculifolius*) increased NO_3^- influx in N-starved Arabidopsis plants (Ma et al., 2020). Thus, our data demonstrates that many actors of the NO_3^- transport machinery are highly expressed in the quadruple *hrs1;hho1;hho2;hho3* mutant.

In conclusion, the modification of HHO TF expression has functional consequences on NO_3^- HATS activities, consistent with their role on the transcriptional control on HATS nitrate transporters *NRT2.4*, *NRT2.5*.

Identification of HRS1 direct targets points to a role of Reactive Oxygen Species

To broaden our investigations around this phenomenon, we studied HRS1 direct genome-wide targets in an N-varying context. To this end, we performed HRS1-perturbation using TARGET approach (Transient Assay Reporting Genome-wide Effect of Transcription factors (Bargmann et al., 2013; Medici et al., 2015; Para et al., 2014)), including 3 biological repeats, by using root protoplasts not treated with NO_3^- during the TARGET procedure. We compared these new results with our previously reported HRS1 TARGET data, performed on NO_3^--containing medium (Medici et al., 2015). Both studies were performed in parallel in the exact same conditions and in the same lab. Cycloheximide (CHX) was maintained in the media during the procedure to retrieve only potential direct targets of HRS1. This provided several important insights concerning HRS1 TF activity. First, we retrieved 1050 potential HRS1 direct targets (non-redundant AGI) (see Material and Method for statistics, and Dataset S1 for the gene list). The obtained HRS1 direct targets were subjected to GeneCloud (Krouk et al., 2015) analysis that performs semantic term enrichment investigation on gene lists (Fig. 5A). This revealed that HRS1 controls a highly coherent group of genes, function-wise. Very strikingly, terms related to redox function (oxidation, peroxide, reductase, oxygen) were highly overrepresented in this list of genes controlled by HRS1 (Fig. 5A, Dataset S1).

A clustering analysis revealed 12 different modes of gene regulation by HRS1 in combination with NO_3^- (Fig. 5B, Dataset S1). Interestingly, the expression of the vast majority (86%) of HRS1 direct genome-wide targets is dependent on the NO_3^- context (Fig. 5B). This can be explained by N-related transcriptional, post-transcriptional and post-translational modifications that could affect HRS1 itself or its partners.

Among the 12 clusters of HRS1 target genes, the two NO_3^--insensitive ones are Clusters #5 and #8. Cluster #8 contains genes whose functions were reminiscent of the germination control of HRS1 demonstrated in previous work (Wu et al., 2012) (Fig. 5B). Cluster #5 contains genes with diverse functions including a Chaperone Dnaj-domain protein and a Glutaredoxin. It is noteworthy that most of the HRS1 regulated gene clusters contain genes related to the cell redox state (Fig. 5B). However, the most enriched clusters in redox related genes are cluster #12 and #2. Cluster #2 contains many genes annotated as heat shock protein and heat shock factors. For this cluster, HRS1 plays a role of repressor only when NO_3^- is provided to the protoplasts. On the other hand, cluster #12 contains genes that are repressed by HRS1 only when NO_3^- is not present during the TARGET procedure (Fig. 5B). This cluster contains many redox related genes such as Catalase1, a Ferredoxin, a Thioredoxin, and a Cupredoxin.

In conclusion, this HRS1 TF perturbation analysis in the plant cell-based TARGET system prompted us to investigate below i) the role of ROS in the NSR, ii) the role of ROS in the HRS1-dependent control of NSR. It also illustrates that a TF can greatly modify its targets according to a nutritional context (Fig. 5).

ROS scavenging molecules are repressors of NSR

To investigate the role of ROS in NSR, we undertook a pharmacological approach. We showed that NSR is strongly repressed if plants are concomitantly treated with ROS-scavenging molecules. In a first experiment, we used a co-treatment with potassium iodide (KI, 5 mM) (Tsukagoshi et al., 2010) and mannitol (5 mM) (Cuin and Shabala, 2007; Shen et al., 1997a, b; Voegele et al., 2005), shown to scavenge H_2O_2 and $^{\bullet}OH$ respectively. This KI-mannitol co-treatment completely abolished the induction of the NSR sentinel genes (Fig. 6A). Then, we investigated the individual as well as the combined effect of KI and mannitol, in parallel with diphenyleniodonium (DPI, NADPH oxidase inhibitor) (Orozco-Cardenas et al., 2001; Tsukagoshi et al., 2010). This experiment confirmed that the inhibition of ROS production has a severe effect on NSR response (Fig. 6B). More precisely, for *NRT2.4* and *NRT2.5*, we recorded that KI and DPI strongly repressed the gene response to N deprivation. For *NRT2.5* and *GDH3,* the mannitol alone seems to also have an effect as it dampens down the transcriptional responses to N depletion. We also found that DMSO may have a potential effect on its own (for *NRT2.5* and *GDH3*) which indeed correlates with the fact that it showed quenching activity on hydroxyl radical ($^{\bullet}OH$) (Franco et al., 2007). However, when DPI treatment was compared to its DMSO mock control, it was itself significantly affecting NSR for the

three sentinel genes (Fig. 6B). These experiments demonstrate that ROS scavenging molecules are affecting plant NSR, and that ROS are an essential activating potential second messenger of NSR.

To further characterize the role of ROS in the control of NSR we studied the effect of *rboh* mutants on NSR response. Indeed, we noticed that a major ROS producing gene (*RBOHC/RHD2*) in plants was a potential direct target of HRS1 since it belongs to cluster #10 (Fig. 5B). We monitored NSR in *rbohc* single and *rbohd;rbohf* double mutants (Fig. S5). As expected *rbohc* mutation (characterized in Fig. S2C) significantly affected the NSR response of *NRT2.4* and *NRT2.5* (Fig. S5). *GDH3* NSR response is affected in *rbohd;rbohf* double mutant. Interestingly H_2O_2 provision reverts mutant phenotype, which strongly suggests that H_2O_2 is necessary to maintain NSR (Fig. S5).

HHO TFs repress NSR through a direct and indirect mechanisms

Given that i) HRS1 regulates ROS related genes (Fig. 5); and ii) ROS production seems to be important for NSR (Fig. 6); and iii) HRS1 and HHOs are themselves important regulators of NSR (Figs. 1, 2); we wanted to investigate if the NSR control by HRS1 could have some branch being ROS-dependent or, if it was a direct regulation. To do this we set up two types of experiments:

-First, we demonstrated that the regulation of *NRT2.4* and *NRT2.5* loci happens through the potential binding of HRS1 to the promoter of these genes (Fig. S6). To this end, we identified a new potential HRS1 DNA-binding element by running the MEME algorithm (Bailey et al., 2009) on the 500 bp upstream sequences of the most repressed HRS1 genes in the TARGET analysis (List from repressed direct targets in (Medici et al., 2015)). This new HRS1 cis-element uncovered contains the GANNNTCTNGA consensus that resembles the consensus motif of HHO2 and HHO3 revealed by DAP-seq in the work by(O'Malley et al., 2016) (Fig. S6A). We used EMSA and competition assays with cold probes to demonstrate that HRS1 had a specific affinity for this new motif, and that the conserved cytosine in the sequence is not critical for the DNA-protein recognition, while the distal guanines play a significant role (Figs. S6B-S6D). Interestingly, this HRS1 motif is found two times in each of the promoters of the 3 sentinel genes as well as in *NRT2.1* (Fig. S6E). We thus tested the binding of HRS1 to probes made from the promoter sequences framing the HRS1 binding sites, and validated that HRS1 is able to bind NSR sentinel genes in a promoter context (Figs. S6E-S6G). Our results are strengthened by DAP-seq data (O'Malley et al., 2016), showing that HHOs sub-family binding (Safi et al., 2017) is especially present in the promoter of the *NRT2.4*, *NRT2.5 and GDH3* genes (Fig. S7). Interestingly no specific binding is recorded for KANADI2 or bZIP16 being respectively: a G2-like TF as well but not in the same sub-family (Safi et al., 2017), or a bZIP (different TF family).

Taken together, DAP-seq (Fig. S7), EMSA (Fig. S6) and TARGET data (Fig. S1A) as well as over-expression approach (Figs. 1, S1B) and mutant phenotypes (Figs. 1-4, S1B), strongly suggest that HRS1 and its homolog genes directly repress the NSR sentinel genes. Very recent results (Kiba et al., 2018) (Maeda et al., 2018) demonstrated that this HRS1-DNA binding occurs using the Yeast-1-Hybrid system and promoter GUS transactivation in plants. This provides a very good external validation of our results and *vice versa*.

-Second, we wanted to test if the HHO-related phenotypes could also be explained by a default in a ROS production and/or accumulation. To this aim, by using Amplex® Red measurements (Chakraborty et al., 2016; Shin et al., 2005; Shin and Schachtman, 2004), we demonstrated that N depletion early (within 6 hours) triggers ROS accumulation in root tissues of WT plants consistent with previous observations (Shin et al., 2005). We also found that this accumulation is lost in the 35S:HRS1 plants and reduced in the 35S:HHO1 genotype validating a role of these TFs in the control of ROS accumulation in plants following N provision (Fig. 7A). Interestingly, the quadruple *hrs1;hho1;hho2;hho3* mutant does not display any ROS accumulation changes in these conditions (Fig. 7A), which could be explained by; i) a modification of their ROS scavenging processes (verified there below), or ii) by referring to the NO_3^- transport phenotypes. Indeed nitrate transport related phenotypes of the HHOs over-expressors are displayed in –N conditions (Fig. 1) and the molecular phenotypes of the mutants are manifested in the +N conditions (Fig. 2B). Thus, we rationalized that it might be the same with ROS-related phenotypes in the *hrs1/hho* mutants.

As we observed that ROS accumulate early in response to N starvation (Fig. 7A), we decided to treat the double and quadruple *hrs1;hho1;hho2;hho3* mutants with KI-mannitol in this context (Fig. 7B). We found that ROS scavenging treatment indeed represses NSR sentinel genes in the *hrs1/hho* mutants to almost the level of WT, totally abolishing the NSR and the mutant phenotype (Fig. 7B). These results show that ROS scavenging agents are able to overcome the mutant phenotype.

We then decided to further analyze the ROS-related mutant phenotypes in –N → +N transfer conditions (Fig. 8A). First, we measured the Ascorbate Peroxidase (APX), glutathione peroxidase (GPX) and Glutathione Reductase activities (GR) in plants (WT and quadruple *hrs1;hho1;hho2;hho3* mutant) grown for 4 weeks on +N (1 mM NH_4NO_3) then transferred to either +N (5 mM KNO_3) or –N (5 mM KCl mock control) for 3 days and finally treated with 5 mM KNO_3 for 3 hours (Fig. 8A). We recorded that N provision to plant pretreated with +N conditions did not change ROS scavenging activities. However, when plants are treated with N after an N starvation period, the quadruple *hrs1;hho1;hho2;hho3* mutant displays a significantly higher activity of APX and GPX (~ 2 fold)

compared to WT plants. This marks a probable hydrogen peroxide (H_2O_2) detoxification program launch, being enhanced in the *hho* mutant as compared to WT (Fig. 8A). This provides also a probable explanation on mild phenotypes recorded in the *hho* mutant for H_2O_2 contents (Fig. 7A).

To continue our study of the quadruple *hrs1;hho1;hho2;hho3* mutant, we performed ROS staining using DAB (3,3'-Diaminobenzidine) and NBT (Nitroblue Tetrazolium) dyes. Notwithstanding that DAB did not yield reproducible results, we observed with NBT staining a strong deviation from the WT in the shoots of the quadruple mutant (Fig. 8B). On N containing media (steady state N provision), we observed that a very weak coloration in the quadruple mutant, supposedly marking a lower accumulation of superoxide ($O_2^{\bullet-}$) or potentially higher detoxification activity. Although unlike our expectation the Amplex® Red and DAB assays did not show a significant increase in the mutant H_2O_2 content, the concomitant enhanced peroxidase (APX and GPX) activities (Fig. 8A) can simply explain this distorted response. The higher scavenging activity may redress the rapid increase of H_2O_2 content to normal (Fig. 7A) while on the other hand, it may deplete the initially normal level of $O_2^{\bullet-}$ (Fig. 8A). Further studies will be necessary to decipher this complex ROS species dynamics.

Interestingly, these above observations are consistent with our over-expression of HHOs in the cell-based TARGET assay (Fig. 5B). Indeed, as stated above, the major cluster of HHO-regulated genes harboring a very high enrichment for ROS-related genes is cluster #2 (Fig. 5B). This cluster contains genes being induced by NO_3^- in -DEX conditions and repressed upon HRS1 nucleus translocation (+NO_3^-, +DEX). This result is exactly what we observe in whole plants. That is N provision triggers ROS accumulation to be repressed in the over-expressors (Fig. 7A). We also measured mRNA accumulation of ROS related genes predicted to be direct targets of HRS1 (Fig. 5) in the quadruple mutant in different N conditions. Results in Fig. S8 show that the *hho* quadruple mutation significantly affects ROS-related genes including (NADPH oxidase, catalases, MDAR…) in an N varying context. Finally, we retrieved key signature genes of the ROS response (different ROS species) defined by a meta-analysis (Vaahtera et al., 2014). To evaluate the control of HRS1 on ROS signature genes, we clustered the expression profile of this gene list and plotted: i) if the gene reports the action of hydrogen peroxide, singlet oxygen, superoxide, or ozone, ii) if the gene is controlled by NO_3^-, HRS1 nuclear entrance (DEX), or the interaction of both (Fig. 8C). This analysis pointed again to the fact that NO_3^-, HRS1 and their combinations influence ROS signature genes for hydrogen peroxide (4 genes), singlet oxygen (3 genes), superoxide (1 gene) (Fig. 8C). Despite the efforts to define ROS specific markers (Gadjev et al., 2006; Rosenwasser et al., 2013), the highly transformable nature of ROS species prevents us from making strong conclusions. However, these

results are in accordance with our *in planta* observations and are another argument showing that HRS1/HHOs are involved in the control of ROS homeostasis in Arabidopsis.

In summary, we show that members of the HHO transcription factor family directly control NSR sentinels (Figs. 1, 2, S6, S7). We also report that upon N starvation, ROS are produced and participate in NSR activation. To a certain extent, ROS accumulation can also explain phenotypes observed in *HHO*-affected genotypes. Thus, we conclude that HRS1 and HHO1 are able to reduce ROS accumulation and potentially repress NSR through a parallel ROS-dependent branch of this signaling pathway (Figs 7, 8, S8).

DISCUSSION

To date the role of ROS as a potential messenger in NSR was hypothesized by several groups (Krapp et al., 2011; Shin et al., 2005) but, to our knowledge, never formally demonstrated. Previously, Shin and Schachtman (2004) demonstrated that upon K starvation, ROS accumulation through the action of RHD2 (NADPH-oxidase) was important to sustain the full transcriptional activation of K^+ transporters. The same group (Shin et al., 2005) also demonstrated that –P, and –N treatments trigger the production of ROS. However, the direct role of ROS in the NSR was so far elusive. In the current work, we present evidence that preventing the production and/or accumulation of ROS during N starvation strongly represses the response of the NSR sentinel genes (Figs 6, 7B, S5). Taken together, these above-mentioned research (Krapp et al., 2011; Shin et al., 2005; Shin and Schachtman, 2004) and others (Balzergue et al., 2017; Hoehenwarter et al., 2016; Mora-Macias et al., 2017; Muller et al., 2015), strongly support that ROS are potential central hubs of the nutrient starvation responses. Because plants are able to distinguish between the different nutritional deprivations, the next challenge will be to understand how is the nutritional specificity of ROS production detected by cells? How is the plant able to detect the ROS signal coming from N rather than a K deficiency? Some clue probably lies into the tissular and cellular specificity of ROS production (Shin et al., 2005). Different types of ROS might presumably have different outcomes with regards to NSR. For instance, whereas H_2O_2 induces *NRT2.1* expression (Bellegarde et al., 2019), nitric oxide ($^{\bullet}NO$) on the other hand inhibits it (Frungillo et al., 2014). Besides their type, ROS subcellular origin might also determine the specificity of each pathway (He et al., 2018). It is noteworthy that H_2O_2 can directly pass from chloroplasts to the nucleus to regulate gene expression (Exposito-

Rodriguez et al., 2017). In addition, ROS not only induce chloroplasts relocalization towards the nucleus (Ding et al., 2019), but also stromule formation leading to the development of direct nucleo chloroplastic interaction (Caplan et al., 2015). Can the plastids sense a lack of N and then increase accordingly their ROS production? N assimilation indeed occurs in the plastids where NO_2^- can enter to be reduced on NH_4^+ and produce amino acids. Many studies revealed an interconnection between C (Carbon) and N status in plants (Malamy and Ryan, 2001) (Coruzzi and Zhou, 2001) (Gutierrez et al., 2007) (Chen et al., 2016) (Ruffel et al., 2020). It is thus worthy to further explore differential response to N deficiency in roots versus shoots. Remarkably we observed a difference in ROS type and accumulation between the roots and the leaves in *hho* mutant (Fig. 7A, 8B). Also unlike our (Fig. 7A) and previous findings (Jung et al., 2018; Shin et al., 2005) which corroborate an increase in H_2O_2 content in N-starved roots, H_2O_2 level was rather slightly decreased in leaves after N starvation (Bieker et al., 2019). Besides, roots and shoots respond differentially to ROS (ozone) treatment (Evans et al., 2005). Recently, it was proposed that ROS might be the integrator that connects N and C signaling (Chaput et al., 2020).

One could also consider that ROS production is an independent and unspecific branch enhancing any kind of nutrient deficiencies whose specificities are encoded by genetic factors (as for Phosphate starvation response (PSR), (Puga et al., 2014)). Those genetic specificities can largely explain why P starvation enhances *HRS1/HHO* expression while N starvation has a repressive effect on their expression, although ROS are being produced in both cases (Maeda et al., 2018; Ueda et al., 2020). Several studies have revealed crosstalk between N and P signaling and that NSR and PSR are tightly interconnected (Hu and Chu, 2020; Kiba et al., 2018; Maeda et al., 2018; Medici et al., 2015; Medici et al., 2019; Ueda et al., 2020). However, more investigations are needed in order to understand for example how ROS are perceived during a combined N and P depletion? But also what are the molecular players and events involved downstream of ROS production in response to nutrient deficiency?

Regarding the NSR, the answer might consist of CC-type glutaredoxins. Remarkably, two independent studies have recently reported that members of CC-type glutaredoxins (aka ROXYs) are differentially expressed in response to variable availability of nitrate (Jung et al., 2018; Patterson et al., 2015). Intriguingly, these ROXY members reveal opposite responses not only to nitrate abundance but also towards oxidative stress (Jung et al., 2018). In other words, ROXYs can be classified in two groups: while the first class which is induced by NO_3^- and repressed by ROS, repress *NRT2* expression, the second that is induced by N starvation and ROS, induces in its turn *NRT2* expression (Jung et al., 2018; Patterson et al., 2015). Rouhier et al. (2008) suggested that different

structural and biochemical properties and therefore different functions of GRX in plants, are the predictable result of their huge number compared to other organisms and of the low conservation of their sequences, particularly around the active site. These remarkable breakthroughs prompted us to investigate how CC-type GRX are regulated by HHO TFs and how this regulation would fit our proposed model. To answer these questions we drilled down through our TARGET data but also through the transcriptomes of *hrs1-hho1* double mutant and of the over-expressor lines (Kiba et al., 2018; Medici et al., 2015). Although the two ROXY classes respond differently to NO_3^- and ROS, some of them are regulated by HHOs in a way that promotes the same fate, namely *NRT2* repression. For example, ROXY15 (GRXS8) and 17 (GRXS6) which act as repressors of *NRT2*, are upregulated by HHOs. On the other hand, the *NRT2* activators ROXY8 (GRXC14) and 9 (GRXC13/CEPD2) are repressed by HHOs. Together, our observations shed light on a new mechanism by which HHO TFs regulate *NRT2* expression and which in its turn strengthens our initial model that the nitrate-induced HHOs repress NSR directly by regulating *NRT2* activity but also indirectly *via* ROS inhibition. With these new findings we gained insight into how ROS might affect NSR marker expression as ROXYs are most likely to be the mediators of ROS signaling in this pathway. It is well established that GRX are involved in oxidative stress responses mostly *via* reducing disulfide bonds of their target proteins (Rouhier et al., 2008). Jung et al. (2018) proposed that similar mechanisms might be used by ROXYs in order to adapt TGA1/4 TF activity. Indeed, those redox-sensitive TFs (Despres et al., 2003) are not only known to be regulators of the PNR by controlling *NRT2.1/NRT2.2* expression (Alvarez et al., 2019; Alvarez et al., 2014), but also to interact with many ROXY members (Li et al., 2009; Murmu et al., 2010; Ndamukong et al., 2007; Zander et al., 2012).

The second factor found in this work, to be a strong regulator of NSR sentinel genes is the transcription factor HRS1. These findings are coherent with recent independent investigations (Kiba et al., 2018; Maeda et al., 2018). HRS1 was previously found to control the P response of primary root development (Liu et al., 2009; Medici et al., 2015) and to control germination *via* an ABA dependent pathway (Wu et al., 2012). HRS1 and its close HHO homolog genes are also very well known to be among the most NO_3^--regulated genes in Arabidopsis (Canales et al., 2014; Krouk et al., 2010b; Wang et al., 2004). The very strong control of HHOs by NO_3^- seems to be important for its functions. Previously, we showed that HRS1 NO_3^- regulation is necessary to integrate the NO_3^- and the PO_4^{3-} signal and to trigger appropriate primary root response (Medici et al., 2015). Herein, we show by TF perturbation *in planta* (over-expressors, mutants) or in plant cells (TARGET), and by DNA-binding assays (EMSA, and DAP-seq), that HRS1 directly represses *NRT2.4*, *NRT2.5* genes. These genes are activated upon N starvation to retrieve NO_3^- traces in the soil solution. Thus, it seems critical for the plant to repress them (by HRS1/HHO TF activity) when NO_3^- is provided to N-starved

plants (Fig. 2). In this work, we generated a genotype missing four HHOs (HRS1, HHO1, HHO2, HHO3). This genotype is unable to fully repress the *NRT2.4* and *NRT2.5* loci (Kiba et al., 2012; Lezhneva et al., 2014). These four mutations lead to an important enhancement of HATS activity (~2.5 fold at 100 µM of external NO_3^-), with a very obvious growth enhancement (Fig. 4). To our knowledge this opens original perspectives to develop genotypes with increased transport capacities in crops, and improve NUE with potential long-term impact on global warming. In the same perspective, a very recent study showed that N-deficiency-induced *OsNLP1* enhances NUE and plant growth by upregulating multiple N uptake and assimilation genes (Alfatih et al., 2020). This includes genes involved in NSR and NO_3^- transport (*NRT2.4*, *NRT2.1*, *NRT1.1*). Based on these inputs, one can postulate that HHOs might also regulate NSR via repressing *NLP1* especially that its promoter is recognized *in vivo* by HHO2 (Kiba et al., 2018).

In conclusion, the model that we propose (Fig. 9) defines two new kinds of molecular actors (the TFs HRS1/HHOs and ROS) in the control of plant NSR (+N → -N). We show that ROS are produced upon NSR and that this response production is necessary for NSR sentinel gene activation. We also show that HRS1 and HHO1 i) control ROS accumulation in response to NSR, ii) and directly repress NSR sentinel genes (*NRT2.4* and *NRT2.5*).

AUTHOR CONTRIBUTIONS

GK, BL, and GC, designed the project.

AS, AM, WS, FM, ACV, AMC, JL, and GK performed the experiments and analyzed the data.

AS, SR, FG, HR, BL, and GK contributed to the study design during the project course.

GK and AS wrote the manuscript with revision from all the authors.

DATA AVAILABILITY

All data and materials will be made available to researchers upon request.

ACKNOWLEDGMENTS

ROS-related enzymatic activities were measured by the Biochemistry Phenotyping Platform (PPB, at CIRAD-AGAP, Montpellier FR). We are very thankful to Dr. Alexandre Martiniere for sharing NADPH oxidase mutants.

REFERENCES

Alboresi A, Gestin C, Leydecker MT, Bedu M, Meyer C, Truong HN. 2005. Nitrate, a signal relieving seed dormancy in Arabidopsis. Plant, Cell & Environment **28**, 500-512.

Alfatih A, Wu J, Zhang ZS, Xia JQ, Jan SU, Yu LH, Xiang CB. 2020. Rice NIN-LIKE PROTEIN 1 rapidly responds to nitrogen deficiency and improves yield and nitrogen use efficiency. Journal of Experimental Botany **71**, 6032-6042.

Alvarez JM, Moyano TC, Zhang T, Gras DE, Herrera FJ, Araus V, O'Brien JA, Carrillo L, Medina J, Vicente-Carbajosa J, Jiang J, Gutierrez RA. 2019. Local Changes in Chromatin Accessibility and Transcriptional Networks Underlying the Nitrate Response in Arabidopsis Roots. Molecular Plant **12**, 1545-1560.

Alvarez JM, Riveras E, Vidal EA, Gras DE, Contreras-Lopez O, Tamayo KP, Aceituno F, Gomez I, Ruffel S, Lejay L, Jordana X, Gutierrez RA. 2014. Systems approach identifies TGA1 and TGA4 transcription factors as important regulatory components of the nitrate response of Arabidopsis thaliana roots. The Plant Journal **80**, 1-13.

Alvarez JM, Schinke AL, Brooks MD, Pasquino A, Leonelli L, Varala K, Safi A, Krouk G, Krapp A, Coruzzi GM. 2020. Transient genome-wide interactions of the master transcription factor NLP7 initiate a rapid nitrogen-response cascade. Nature Communications **11**, 1157.

Araus V, Vidal EA, Puelma T, Alamos S, Mieulet D, Guiderdoni E, Gutierrez RA. 2016. Members of BTB Gene Family of Scaffold Proteins Suppress Nitrate Uptake and Nitrogen Use Efficiency. Plant Physiology **171**, 1523-1532.

Bailey TL, Boden M, Buske FA, Frith M, Grant CE, Clementi L, Ren J, Li WW, Noble WS. 2009. MEME SUITE: tools for motif discovery and searching. Nucleic Acids Research **37**, W202-208.

Balzergue C, Dartevelle T, Godon C, Laugier E, Meisrimler C, Teulon JM, Creff A, Bissler M, Brouchoud C, Hagege A, Muller J, Chiarenza S, Javot H, Becuwe-Linka N, David P, Peret B, Delannoy E, Thibaud MC, Armengaud J, Abel S, Pellequer JL, Nussaume L, Desnos T. 2017. Low phosphate activates STOP1-ALMT1 to rapidly inhibit root cell elongation. Nature Communications **8**, 15300.

Bargmann BO, Marshall-Colon A, Efroni I, Ruffel S, Birnbaum KD, Coruzzi GM, Krouk G. 2013. TARGET: a transient transformation system for genome-wide transcription factor target discovery. Molecular Plant **6**, 978-980.

Bellegarde F, Maghiaoui A, Boucherez J, Krouk G, Lejay L, Bach L, Gojon A, Martin A. 2019. The Chromatin Factor HNI9 and ELONGATED HYPOCOTYL5 Maintain ROS Homeostasis under High Nitrogen Provision. Plant Physiology **180**, 582-592.

Bieker S, Riester L, Doll J, Franzaring J, Fangmeier A, Zentgraf U. 2019. Nitrogen Supply Drives Senescence-Related Seed Storage Protein Expression in Rapeseed Leaves. Genes (Basel) **10**.

Canales J, Moyano TC, Villarroel E, Gutierrez RA. 2014. Systems analysis of transcriptome data provides new hypotheses about Arabidopsis root response to nitrate treatments. Frontiers in Plant Science **5**, 22.

Caplan JL, Kumar AS, Park E, Padmanabhan MS, Hoban K, Modla S, Czymmek K, Dinesh-Kumar SP. 2015. Chloroplast Stromules Function during Innate Immunity. Developmental Cell **34**, 45-57.

Castaings L, Camargo A, Pocholle D, Gaudon V, Texier Y, Boutet-Mercey S, Taconnat L, Renou JP, Daniel-Vedele F, Fernandez E, Meyer C, Krapp A. 2009. The nodule inception-like protein 7 modulates nitrate sensing and metabolism in Arabidopsis. The Plant Journal **57**, 426-435.

Castro Marin I, Loef I, Bartetzko L, Searle I, Coupland G, Stitt M, Osuna D. 2010. Nitrate regulates floral induction in Arabidopsis, acting independently of light, gibberellin and autonomous pathways. Planta.

Chakraborty S, Hill AL, Shirsekar G, Afzal AJ, Wang GL, Mackey D, Bonello P. 2016. Quantification of hydrogen peroxide in plant tissues using Amplex Red. Methods **109**, 105-113.
Chaput V, Martin A, Lejay L. 2020. Redox metabolism: the hidden player in carbon and nitrogen signaling? Journal of Experimental Botany **71**, 3816-3826.
Chen X, Yao Q, Gao X, Jiang C, Harberd NP, Fu X. 2016. Shoot-to-Root Mobile Transcription Factor HY5 Coordinates Plant Carbon and Nitrogen Acquisition. Current Biology **26**, 640-646.
Choudhury FK, Rivero RM, Blumwald E, Mittler R. 2017. Reactive oxygen species, abiotic stress and stress combination. The Plant Journal **90**, 856-867.
Clarkson DT, Gojon A, Saker LR, Wiersema PK, Purves JV, Tillard P, Arnold GM, Paams AJM, Waalburg W, Stulen I. 1996. Nitrate and ammonium influxes in soybean (*Glycine max*) roots: Direct comparison of ^{13}N and ^{15}N tracing. Plant, Cell & Environment **19**, 859-868.
Coruzzi G, Zhou L. 2001. Carbon and nitrogen sensing and signaling in plants: emerging 'matrix effects'. Current Opinion in Plant Biology **4**, 247-253.
Crawford NM, Glass ADM. 1998. Molecular and physiological aspects of nitrate uptake in plants. Trends in Plant Science **3**, 389-395.
Cuin TA, Shabala S. 2007. Compatible solutes reduce ROS-induced potassium efflux in Arabidopsis roots. Plant, Cell & Environment **30**, 875-885.
Curtis MD, Grossniklaus U. 2003. A gateway cloning vector set for high-throughput functional analysis of genes in planta. Plant Physiology **133**, 462-469.
Despres C, Chubak C, Rochon A, Clark R, Bethune T, Desveaux D, Fobert PR. 2003. The Arabidopsis NPR1 disease resistance protein is a novel cofactor that confers redox regulation of DNA binding activity to the basic domain/leucine zipper transcription factor TGA1. The Plant Cell **15**, 2181-2191.
Ding X, Jimenez-Gongora T, Krenz B, Lozano-Duran R. 2019. Chloroplast clustering around the nucleus is a general response to pathogen perception in Nicotiana benthamiana. Molecular Plant Pathology **20**, 1298-1306.
Evans NH, McAinsh MR, Hetherington AM, Knight MR. 2005. ROS perception in Arabidopsis thaliana: the ozone-induced calcium response. The Plant Journal **41**, 615-626.
Exposito-Rodriguez M, Laissue PP, Yvon-Durocher G, Smirnoff N, Mullineaux PM. 2017. Photosynthesis-dependent H2O2 transfer from chloroplasts to nuclei provides a high-light signalling mechanism. Nature Communications **8**, 49.
Forde BG, Walch-Liu P. 2009. Nitrate and glutamate as environmental cues for behavioural responses in plant roots. Plant, Cell & Environment **32**, 682-693.
Foyer CH, Noctor G. 2013. Redox signaling in plants. Antioxidants and Redox Signaling **18**, 2087-2090.
Franco R, Panayiotidis MI, Cidlowski JA. 2007. Glutathione depletion is necessary for apoptosis in lymphoid cells independent of reactive oxygen species formation. Journal of Biological Chemistry **282**, 30452-30465.
Frungillo L, Skelly MJ, Loake GJ, Spoel SH, Salgado I. 2014. S-nitrosothiols regulate nitric oxide production and storage in plants through the nitrogen assimilation pathway. Nature Communications **5**, 5401.
Gadjev I, Vanderauwera S, Gechev TS, Laloi C, Minkov IN, Shulaev V, Apel K, Inze D, Mittler R, Van Breusegem F. 2006. Transcriptomic footprints disclose specificity of reactive oxygen species signaling in Arabidopsis. Plant Physiology **141**, 436-445.
Gansel X, Munos S, Tillard P, Gojon A. 2001. Differential regulation of the NO_3^- and NH_4^+ transporter genes *AtNrt2.1* and *AtAmt1.1* in Arabidopsis: relation with long-distance and local controls by N status of the plant. The Plant Journal **26**, 143-155.
Gautrat P, Laffont C, Frugier F, Ruffel S. 2020. Nitrogen Systemic Signaling: From Symbiotic Nodulation to Root Acquisition. Trends in Plant Science.
Gruber BD, Giehl RF, Friedel S, von Wiren N. 2013. Plasticity of the Arabidopsis root system under nutrient deficiencies. Plant Physiology **163**, 161-179.

Guan P, Ripoll JJ, Wang R, Vuong L, Bailey-Steinitz LJ, Ye D, Crawford NM. 2017. Interacting TCP and NLP transcription factors control plant responses to nitrate availability. Proceedings of the National Academy of Sciences, USA **114**, 2419-2424.
Gutierrez RA, Lejay LV, Dean A, Chiaromonte F, Shasha DE, Coruzzi GM. 2007. Qualitative network models and genome-wide expression data define carbon/nitrogen-responsive molecular machines in Arabidopsis. Genome Biology **8**, R7.
Han M, Okamoto M, Beatty PH, Rothstein SJ, Good AG. 2015. The Genetics of Nitrogen Use Efficiency in Crop Plants. Annual Review of Genetics **49**, 269-289.
He H, Van Breusegem F, Mhamdi A. 2018. Redox-dependent control of nuclear transcription in plants. Journal of Experimental Botany **69**, 3359-3372.
Ho CH, Lin SH, Hu HC, Tsay YF. 2009. CHL1 functions as a nitrate sensor in plants. Cell **138**, 1184-1194.
Hoehenwarter W, Monchgesang S, Neumann S, Majovsky P, Abel S, Muller J. 2016. Comparative expression profiling reveals a role of the root apoplast in local phosphate response. BMC Plant Biology **16**, 106.
Hu B, Chu C. 2020. Nitrogen-phosphorus interplay: old story with molecular tale. New Phytologist **225**, 1455-1460.
Hu HC, Wang YY, Tsay YF. 2009. AtCIPK8, a CBL-interacting protein kinase, regulates the low-affinity phase of the primary nitrate response. The Plant Journal **57**, 264-278.
Jung JY, Ahn JH, Schachtman DP. 2018. CC-type glutaredoxins mediate plant response and signaling under nitrate starvation in Arabidopsis. BMC Plant Biology **18**, 281.
Kiba T, Feria-Bourrellier AB, Lafouge F, Lezhneva L, Boutet-Mercey S, Orsel M, Brehaut V, Miller A, Daniel-Vedele F, Sakakibara H, Krapp A. 2012. The Arabidopsis nitrate transporter NRT2.4 plays a double role in roots and shoots of nitrogen-starved plants. The Plant Cell **24**, 245-258.
Kiba T, Inaba J, Kudo T, Ueda N, Konishi M, Mitsuda N, Takiguchi Y, Kondou Y, Yoshizumi T, Ohme-Takagi M, Matsui M, Yano K, Yanagisawa S, Sakakibara H. 2018. Repression of Nitrogen Starvation Responses by Members of the Arabidopsis GARP-Type Transcription Factor NIGT1/HRS1 Subfamily. The Plant Cell **30**, 925-945.
Kiba T, Krapp A. 2016. Plant Nitrogen Acquisition Under Low Availability: Regulation of Uptake and Root Architecture. Plant & Cell Physiology **57**, 707-714.
Krapp A, Berthome R, Orsel M, Mercey-Boutet S, Yu A, Castaings L, Elftieh S, Major H, Renou JP, Daniel-Vedele F. 2011. Arabidopsis roots and shoots show distinct temporal adaptation patterns toward nitrogen starvation. Plant Physiology **157**, 1255-1282.
Krouk G. 2017. Nitrate signalling: Calcium bridges the nitrate gap. Nature Plants **3**, 17095.
Krouk G, Carre C, Fizames C, Gojon A, Ruffel S, Lacombe B. 2015. GeneCloud Reveals Semantic Enrichment in Lists of Gene Descriptions. Molecular Plant **8**, 971-973.
Krouk G, Crawford NM, Coruzzi GM, Tsay YF. 2010a. Nitrate signaling: adaptation to fluctuating environments. Current Opinion in Plant Biology **13**, 266-273.
Krouk G, Mirowski P, LeCun Y, Shasha DE, Coruzzi GM. 2010b. Predictive network modeling of the high-resolution dynamic plant transcriptome in response to nitrate. Genome Biology **11**, R123.
Leclercq J, Martin F, Sanier C, Clement-Vidal A, Fabre D, Oliver G, Lardet L, Ayar A, Peyramard M, Montoro P. 2012. Over-expression of a cytosolic isoform of the HbCuZnSOD gene in Hevea brasiliensis changes its response to a water deficit. Plant Molecular Biology **80**, 255-272.
Lejay L, Tillard P, Lepetit M, Olive F, Filleur S, Daniel-Vedele F, Gojon A. 1999. Molecular and functional regulation of two NO_3^- uptake systems by N- and C-status of Arabidopsis plants. The Plant Journal **18**, 509-519.
Leran S, Edel KH, Pervent M, Hashimoto K, Corratge-Faillie C, Offenborn JN, Tillard P, Gojon A, Kudla J, Lacombe B. 2015. Nitrate sensing and uptake in Arabidopsis are enhanced by ABI2, a phosphatase inactivated by the stress hormone abscisic acid. Science Signaling **8**, ra43.
Lezhneva L, Kiba T, Feria-Bourrellier AB, Lafouge F, Boutet-Mercey S, Zoufan P, Sakakibara H, Daniel-Vedele F, Krapp A. 2014. The Arabidopsis nitrate transporter

NRT2.5 plays a role in nitrate acquisition and remobilization in nitrogen-starved plants. The Plant Journal **80**, 230-241.
Li S, Lauri A, Ziemann M, Busch A, Bhave M, Zachgo S. 2009. Nuclear activity of ROXY1, a glutaredoxin interacting with TGA factors, is required for petal development in Arabidopsis thaliana. The Plant Cell **21**, 429-441.
Li Y, Krouk G, Coruzzi GM, Ruffel S. 2014. Finding a nitrogen niche: a systems integration of local and systemic nitrogen signalling in plants. Journal of Experimental Botany.
Liu H, Yang H, Wu C, Feng J, Liu X, Qin H, Wang D. 2009. Overexpressing HRS1 confers hypersensitivity to low phosphate-elicited inhibition of primary root growth in Arabidopsis thaliana. Journal of integrative plant biology **51**, 382-392.
Liu KH, Niu Y, Konishi M, Wu Y, Du H, Sun Chung H, Li L, Boudsocq M, McCormack M, Maekawa S, Ishida T, Zhang C, Shokat K, Yanagisawa S, Sheen J. 2017. Discovery of nitrate-CPK-NLP signalling in central nutrient-growth networks. Nature.
Ma H, Zhao J, Feng S, Qiao K, Gong S, Wang J, Zhou A. 2020. Heterologous Expression of Nitrate Assimilation Related-Protein DsNAR2.1/NRT3.1 Affects Uptake of Nitrate and Ammonium in Nitrogen-Starved Arabidopsis. International Journal of Molecular Sciences **21**.
Ma Q, Tang RJ, Zheng XJ, Wang SM, Luan S. 2015. The calcium sensor CBL7 modulates plant responses to low nitrate in Arabidopsis. Biochemical and Biophysical Research Communications **468**, 59-65.
Maeda Y, Konishi M, Kiba T, Sakuraba Y, Sawaki N, Kurai T, Ueda Y, Sakakibara H, Yanagisawa S. 2018. A NIGT1-centred transcriptional cascade regulates nitrate signalling and incorporates phosphorus starvation signals in Arabidopsis. Nature Communications **9**, 1376.
Malamy JE, Ryan KS. 2001. Environmental regulation of lateral root initiation in Arabidopsis. Plant Physiology **127**, 899-909.
Marchi L, Degola F, Polverini E, Terce-Laforgue T, Dubois F, Hirel B, Restivo FM. 2013. Glutamate dehydrogenase isoenzyme 3 (GDH3) of Arabidopsis thaliana is regulated by a combined effect of nitrogen and cytokinin. Plant Physiology and Biochemistry **73**, 368-374.
Marchive C, Roudier F, Castaings L, Brehaut V, Blondet E, Colot V, Meyer C, Krapp A. 2013. Nuclear retention of the transcription factor NLP7 orchestrates the early response to nitrate in plants. Nature Communications **4**, 1713.
Medici A, Krouk G. 2014. The primary nitrate response: a multifaceted signalling pathway. Journal of Experimental Botany **65**, 5567-5576.
Medici A, Marshall-Colon A, Ronzier E, Szponarski W, Wang R, Gojon A, Crawford NM, Ruffel S, Coruzzi GM, Krouk G. 2015. AtNIGT1/HRS1 integrates nitrate and phosphate signals at the Arabidopsis root tip. Nature Communications **6**, 6274.
Medici A, Szponarski W, Dangeville P, Safi A, Dissanayake IM, Saenchai C, Emanuel A, Rubio V, Lacombe B, Ruffel S, Tanurdzic M, Rouached H, Krouk G. 2019. Identification of Molecular Integrators Shows that Nitrogen Actively Controls the Phosphate Starvation Response in Plants. The Plant Cell **31**, 1171-1184.
Menz J, Li Z, Schulze WX, Ludewig U. 2016. Early nitrogen-deprivation responses in Arabidopsis roots reveal distinct differences on transcriptome and (phospho-) proteome levels between nitrate and ammonium nutrition. The Plant Journal **88**, 717-734.
Mora-Macias J, Ojeda-Rivera JO, Gutierrez-Alanis D, Yong-Villalobos L, Oropeza-Aburto A, Raya-Gonzalez J, Jimenez-Dominguez G, Chavez-Calvillo G, Rellan-Alvarez R, Herrera-Estrella L. 2017. Malate-dependent Fe accumulation is a critical checkpoint in the root developmental response to low phosphate. Proceedings of the National Academy of Sciences, USA **114**, E3563-E3572.
Muller J, Toev T, Heisters M, Teller J, Moore KL, Hause G, Dinesh DC, Burstenbinder K, Abel S. 2015. Iron-dependent callose deposition adjusts root meristem maintenance to phosphate availability. Developmental Cell **33**, 216-230.
Murmu J, Bush MJ, DeLong C, Li S, Xu M, Khan M, Malcolmson C, Fobert PR, Zachgo S, Hepworth SR. 2010. Arabidopsis basic leucine-zipper transcription factors TGA9 and TGA10 interact with floral glutaredoxins ROXY1 and ROXY2 and are redundantly required for anther development. Plant Physiology **154**, 1492-1504.

Ndamukong I, Abdallat AA, Thurow C, Fode B, Zander M, Weigel R, Gatz C. 2007. SA-inducible Arabidopsis glutaredoxin interacts with TGA factors and suppresses JA-responsive PDF1.2 transcription. The Plant Journal **50**, 128-139.
Noctor G, Reichheld JP, Foyer CH. 2018. ROS-related redox regulation and signaling in plants. Seminars in Cell & Developmental Biology **80**, 3-12.
O'Brien JA, Vega A, Bouguyon E, Krouk G, Gojon A, Coruzzi G, Gutierrez RA. 2016. Nitrate Transport, Sensing, and Responses in Plants. Molecular Plant **9**, 837-856.
O'Malley RC, Huang SS, Song L, Lewsey MG, Bartlett A, Nery JR, Galli M, Gallavotti A, Ecker JR. 2016. Cistrome and Epicistrome Features Shape the Regulatory DNA Landscape. Cell **165**, 1280-1292.
Obertello M, Krouk G, Katari MS, Runko SJ, Coruzzi GM. 2010. Modeling the global effect of the basic-leucine zipper transcription factor 1 (bZIP1) on nitrogen and light regulation in Arabidopsis. BMC Systems Biology **4**, 111.
Ohkubo Y, Tanaka M, Tabata R, Ogawa-Ohnishi M, Matsubayashi Y. 2017. Shoot-to-root mobile polypeptides involved in systemic regulation of nitrogen acquisition. Nature Plants **3**, 17029.
Okamoto M, Vidmar JJ, Glass AD. 2003. Regulation of NRT1 and NRT2 gene families of *Arabidopsis thaliana*: responses to nitrate provision. Plant & Cell Physiology **44**, 304-317.
Orozco-Cardenas ML, Narvaez-Vasquez J, Ryan CA. 2001. Hydrogen peroxide acts as a second messenger for the induction of defense genes in tomato plants in response to wounding, systemin, and methyl jasmonate. The Plant Cell **13**, 179-191.
Ota R, Ohkubo Y, Yamashita Y, Ogawa-Ohnishi M, Matsubayashi Y. 2020. Shoot-to-root mobile CEPD-like 2 integrates shoot nitrogen status to systemically regulate nitrate uptake in Arabidopsis. Nature Communications **11**, 641.
Para A, Li Y, Marshall-Colon A, Varala K, Francoeur NJ, Moran TM, Edwards MB, Hackley C, Bargmann BO, Birnbaum KD, McCombie WR, Krouk G, Coruzzi GM. 2014. Hit-and-run transcriptional control by bZIP1 mediates rapid nutrient signaling in Arabidopsis. Proceedings of the National Academy of Sciences, USA **111**, 10371-10376.
Patterson K, Walters L, Cooper A, Olvera J, Rosas M, Rasmusson A, Escobar M. 2015. Nitrate-regulated glutaredoxins control Arabidopsis thaliana primary root growth. Plant Physiology.
Poitout A, Martiniere A, Kucharczyk B, Queruel N, Silva-Andia J, Mashkoor S, Gamet L, Varoquaux F, Paris N, Sentenac H, Touraine B, Desbrosses G. 2017. Local signalling pathways regulate the Arabidopsis root developmental response to Mesorhizobium loti inoculation. Journal of Experimental Botany **68**, 1199-1211.
Puga MI, Mateos I, Charukesi R, Wang Z, Franco-Zorrilla JM, de Lorenzo L, Irigoyen ML, Masiero S, Bustos R, Rodriguez J, Leyva A, Rubio V, Sommer H, Paz-Ares J. 2014. SPX1 is a phosphate-dependent inhibitor of PHOSPHATE STARVATION RESPONSE 1 in Arabidopsis. Proceedings of the National Academy of Sciences, USA **111**, 14947-14952.
Rahayu YS, Walch-Liu P, Neumann G, Romheld V, von Wiren N, Bangerth F. 2005. Root-derived cytokinins as long-distance signals for NO_3^--induced stimulation of leaf growth. Journal of Experimental Botany **56**, 1143-1152.
Ristova D, Carre C, Pervent M, Medici A, Kim GJ, Scalia D, Ruffel S, Birnbaum K, Lacombe B, Busch W, Coruzzi G, Krouk G. 2016. Combinatorial interaction network of transcriptomic and phenotypic responses to nitrogen and hormones in the Arabidopsis thaliana root. Science Signaling **9**.
Riveras E, Alvarez JM, Vidal EA, Oses C, Vega A, Gutierrez RA. 2015. The Calcium Ion Is a Second Messenger in the Nitrate Signaling Pathway of Arabidopsis. Plant Physiology **169**, 1397-1404.
Rosenwasser S, Fluhr R, Joshi JR, Leviatan N, Sela N, Hetzroni A, Friedman H. 2013. ROSMETER: a bioinformatic tool for the identification of transcriptomic imprints related to reactive oxygen species type and origin provides new insights into stress responses. Plant Physiology **163**, 1071-1083.
Rouhier N, Lemaire SD, Jacquot JP. 2008. The role of glutathione in photosynthetic organisms: emerging functions for glutaredoxins and glutathionylation. Annual Review of Plant Biology **59**, 143-166.

Rubin G, Tohge T, Matsuda F, Saito K, Scheible WR. 2009. Members of the LBD family of transcription factors repress anthocyanin synthesis and affect additional nitrogen responses in Arabidopsis. The Plant Cell **21**, 3567-3584.
Ruffel S, Chaput V, Przybyla-Toscano J, Fayos I, Ibarra C, Moyano T, Fizames C, Tillard P, O'Brien JA, Gutierrez RA, Gojon A, Lejay L. 2020. Genome-wide Analysis In Response to Nitrogen and Carbon Identifies Regulators for root AtNRT2 Transporters. Plant Physiology.
Ruffel S, Krouk G, Ristova D, Shasha D, Birnbaum KD, Coruzzi GM. 2011. Nitrogen economics of root foraging: transitive closure of the nitrate-cytokinin relay and distinct systemic signaling for N supply vs. demand. Proceedings of the National Academy of Sciences, USA **108**, 18524-18529.
Ruffel S, Poitout A, Krouk G, Coruzzi GM, Lacombe B. 2015. Long-distance nitrate signaling displays cytokinin dependent and independent branches. Journal of integrative plant biology.
Safi A, Medici A, Szponarski W, Ruffel S, Lacombe B, Krouk G. 2017. The world according to GARP transcription factors. Current Opinion in Plant Biology **39**, 159-167.
Scheible WR, Gonzalez-Fontes A, Lauerer M, Muller-Rober B, Caboche M, Stitt M. 1997. Nitrate Acts as a Signal to Induce Organic Acid Metabolism and Repress Starch Metabolism in Tobacco. The Plant Cell **9**, 783-798.
Shen B, Jensen RG, Bohnert HJ. 1997a. Increased resistance to oxidative stress in transgenic plants by targeting mannitol biosynthesis to chloroplasts. Plant Physiology **113**, 1177-1183.
Shen B, Jensen RG, Bohnert HJ. 1997b. Mannitol Protects against Oxidation by Hydroxyl Radicals. Plant Physiology **115**, 527-532.
Shin R, Berg RH, Schachtman DP. 2005. Reactive oxygen species and root hairs in Arabidopsis root response to nitrogen, phosphorus and potassium deficiency. Plant & Cell Physiology **46**, 1350-1357.
Shin R, Schachtman DP. 2004. Hydrogen peroxide mediates plant root cell response to nutrient deprivation. Proceedings of the National Academy of Sciences, USA **101**, 8827-8832.
Stitt M. 1999. Nitrate regulation of metabolism and growth. Current Opinion in Plant Biology **2**, 178-186.
Sutton MA, Oenema O, Erisman JW, Leip A, Grinsven HV, Winiwarter W. 2011. Too much of a good thing. Nature **472**, 159-161.
Tabata R, Sumida K, Yoshii T, Ohyama K, Shinohara H, Matsubayashi Y. 2014. Perception of root-derived peptides by shoot LRR-RKs mediates systemic N-demand signaling. Science **346**, 343-346.
Tsukagoshi H, Busch W, Benfey PN. 2010. Transcriptional regulation of ROS controls transition from proliferation to differentiation in the root. Cell **143**, 606-616.
Ueda Y, Kiba T, Yanagisawa S. 2020. Nitrate-inducible NIGT1 proteins modulate phosphate uptake and starvation signalling via transcriptional regulation of SPX genes. The Plant Journal **102**, 448-466.
Vaahtera L, Brosche M, Wrzaczek M, Kangasjarvi J. 2014. Specificity in ROS signaling and transcript signatures. Antioxidants and Redox Signaling **21**, 1422-1441.
Voegele RT, Hahn M, Lohaus G, Link T, Heiser I, Mendgen K. 2005. Possible roles for mannitol and mannitol dehydrogenase in the biotrophic plant pathogen Uromyces fabae. Plant Physiology **137**, 190-198.
Wang R, Tischner R, Gutierrez RA, Hoffman M, Xing X, Chen M, Coruzzi G, Crawford NM. 2004. Genomic analysis of the nitrate response using a nitrate reductase-null mutant of Arabidopsis. Plant Physiology **136**, 2512-2522.
Wang R, Xing X, Wang Y, Tran A, Crawford NM. 2009. A genetic screen for nitrate regulatory mutants captures the nitrate transporter gene NRT1.1. Plant Physiology **151**, 472-478.
Widiez T, El Kafafi el S, Girin T, Berr A, Ruffel S, Krouk G, Vayssieres A, Shen WH, Coruzzi GM, Gojon A, Lepetit M. 2011. High nitrogen insensitive 9 (HNI9)-mediated

systemic repression of root NO3- uptake is associated with changes in histone methylation. Proceedings of the National Academy of Sciences, USA **108**, 13329-13334.
Wu C, Feng J, Wang R, Liu H, Yang H, Rodriguez PL, Qin H, Liu X, Wang D. 2012. HRS1 acts as a negative regulator of abscisic acid signaling to promote timely germination of Arabidopsis seeds. PLoS One **7**, e35764.
Xu N, Wang R, Zhao L, Zhang C, Li Z, Lei Z, Liu F, Guan P, Chu Z, Crawford NM, Wang Y. 2016. The Arabidopsis NRG2 Protein Mediates Nitrate Signaling and Interacts with and Regulates Key Nitrate Regulators. The Plant Cell **28**, 485-504.
Yong Z, Kotur Z, Glass AD. 2010. Characterization of an intact two-component high-affinity nitrate transporter from Arabidopsis roots. The Plant Journal **63**, 739-748.
Zander M, Chen S, Imkampe J, Thurow C, Gatz C. 2012. Repression of the Arabidopsis thaliana jasmonic acid/ethylene-induced defense pathway by TGA-interacting glutaredoxins depends on their C-terminal ALWL motif. Molecular Plant **5**, 831-840.
Zhang X, Henriques R, Lin SS, Niu QW, Chua NH. 2006. Agrobacterium-mediated transformation of Arabidopsis thaliana using the floral dip method. Nature Protocols **1**, 641-646.
Zhao M, Ding H, Zhu JK, Zhang F, Li WX. 2011. Involvement of miR169 in the nitrogen-starvation responses in Arabidopsis. New Phytologist **190**, 906-915.

FIGURE LEGENDS

Fig. 1. HRS1 and HHO1 are repressors of NSR sentinel genes. (A) Root response of *NRT2.4*, *NRT2.5* and *GDH3* to NSR in Columbia, *hrs1;hho1*, 35S:HRS1 genotypes. Plants were grown in sterile hydroponic conditions on N-containing medium for 14 days. At time 0, the medium was shifted to –N conditions for 0, 2, 4, 6 days or +N as a control. **(B)** Root response of *NRT2.4*, *NRT2.5* and *GDH3* to NSR in Columbia WT, 35S:HRS1, 35S:HHO1 genotypes. Plants were grown in sterile hydroponic conditions on N-containing medium for 14 days. Then the medium was shifted to –N conditions for 0, 1, 2, 4, 6 days (the media background was kept unchanged). All transcript levels were quantified by qPCR and normalized to two housekeeping genes (*ACT* and *CLA*), values are means ± s.e.m (n= 4). Asterisks indicate significant differences from WT plants (*P<0.05; **P<0.01; ***P<0.001; Student's t-test).

Fig. 2. HHO subfamily is involved in repressing NSR sentinels after NO_3^- provision.

(A) Phylogenetic tree representing the GARP HHO subfamily. The tree was built as previously described (Safi et al., 2017). **(B)** Root response of *NRT2.4*, *NRT2.5* and *GDH3* to PNR following N starvation in Columbia WT, *hrs1*, *hrs1;hho1, hrs1;hho1;hho2*, *hrs1;hho1;hho2;hho3* genotypes. Plants were grown in sterile hydroponic conditions on full medium for 14 days, subjected to N starvation for 3 days and then resupplied with 0.5 mM NH_4NO_3 for 0 (harvested before treatment), 15 min, 30 min, 1h, 2h, 3h, 4h (the media background was kept unchanged). **(C)** *NRT2.4* expression 2 hours after N supply showing an additive de-repression effect following sequential deletion of *HHO* genes. **(D)** pHRS1:HRS1:GFP is sufficient to complement the quadruple mutant. WT, *hrs1;hho1;hho2;hho3*, *hrs1;hho1;hho2;hho3*;pHRS1:HRS1:GFP line 1 and line 2 (2 independent transformation events) were grown on petri dishes on 0.5 mM of NH_4NO_3 for 12 days. Roots were harvested and transcripts were measured by qPCR. All transcript levels were quantified by qPCR and normalized to two housekeeping genes (*ACT* and *CLA*), values are means ± s.e.m (n= 4). Asterisks indicate significant differences from WT plants (*P<0.05; **P<0.01; ***P<0.001; Student's t-test).

Fig. 3. HRS1 and HHO1 negatively control NO_3^- HATS. (A) NO_3^- uptake is altered in the 35S:HRS1 and in the double mutant *hrs1;hho1*. Plants were grown for 5 weeks on N-containing medium. The medium was then shifted to –N conditions or +N as a control for 1 or 3 weeks. Values are means ± s.e.m (n= 6). **(B)** One week-starved plants were used to quantify NO_3^- HATS and LATS activities as well as high affinity NO_3^- transporter transcript levels. qPCR data were normalized to two housekeeping genes (*ACT* and *CLA*), values are means ± s.e.m (n= 12). NO_3^- uptake measurements were performed on different $^{15}NO_3^-$ concentrations (10, 100, 250 µM, 1 and 5 mM) to evaluate HATS and LATS. Values are means ± s.e.m (n= 6). The experiment was performed exactly as mentioned for (a). Asterisks indicate significant differences from WT plants (*P<0.05; **P<0.01; ***P<0.001; Student's t-test).

Fig. 4. The HHO subfamily represses NO_3^- uptake and growth in +N conditions.

(A) NO_3^- uptake is altered in *hrs1*, *hrs1;hho1*, *hrs1;hho1;hho2* and *hrs1;hho1;hho2;hho3* mutants. Plants were grown for 6 weeks on N-containing non-sterile hydroponics (0.5 mM NH_4NO_3). NO_3^- uptake measurements were performed at 100 µM $^{15}NO_3^-$ to evaluate the HATS. Values are means ± s.e.m (n= 6). Asterisks indicate significant differences from WT plants (*P<0.05; **P<0.01; ***P<0.001; Student's t-test). **(B)** Representative pictures of WT and *hrs1;hho1;hho2;hho3* quadruple mutant, grown on +N conditions, at the day of the uptake experiment show a growth phenotype.

Fig. 5. HRS1 direct genome-wide targets are largely NO_3^--dependent and contain many redox-related genes. TARGET procedure was performed with NO_3^- (data from (Medici et al., 2015)) and without NO_3^- (this work). An ANOVA analysis followed by a Tukey test retrieved 1050 HRS1-regulated genes (ANOVA pval cutoff 0.01, Tukey pval cutoff 0.01, FDR<10%). **(A)** GeneCloud analysis (Krouk et al., 2015) of the 1050 direct targets of HRS1. **(B)** Clustering analysis (Pearson correlation) was performed using MeV software (number of clusters was determined by the FOM method). A selection of over-represented semantic terms is displayed in front of each cluster. Notable redox-related genes are displayed in the right column. The list of each cluster, their related gene list, as well as their respective semantic analysis are provided in Dataset S1.

Fig. 6. ROS are necessary for NSR. (A) Altered response of *NRT2.4*, *NRT2.5* and *GDH3* by KI-mannitol treatment. Plants were grown in sterile hydroponic conditions on N-containing medium for 14 days. Thereafter, the medium was shifted to –N conditions containing or not 5 mM of KI and 5 mM of mannitol for 0, 2, 4, 6 days or +N as a control. **(B)** Altered response of *NRT2.4*, *NRT2.5* and *GDH3* by ROS scavenger treatment. Plants were grown in sterile hydroponic conditions on N-containing medium for 14 days. Then they were transferred to –N or +N conditions for 0, 2, 4 days. In parallel, some of the N-starved plants were treated with 5 mM KI, 5 mM mannitol, combination of both or with 10 µM DPI. DMSO was used as a mock treatment of DPI. All transcript levels were quantified by qPCR and normalized to two housekeeping genes (*ACT* and *CLA*), values are means ± s.e.m (n= 4). Asterisks indicate significant differences from WT plants (*P<0.05; **P<0.01; ***P<0.001; Student's t-test).

Fig. 7. ROS are produced early after nitrogen deprivation, regulated by HRS1 and crucial for NSR. (A) H_2O_2 production after N deprivation. Plants were grown in non-sterile hydroponics for 6 weeks on N-containing medium. Thereafter, the medium was shifted to –N conditions or +N as a control for 6 hours. H_2O_2 accumulation was measured using Amplex® Red (see Material and Methods). Values are means ± s.e.m (n= 6). Different letters means significant differences (Student's t-test, P < 0.05). **(B)** ROS-scavenging treatment represses NSR sentinel genes in *hho* mutants. Plants were grown in sterile hydroponic conditions on N-containing medium for 14 days. They were then N-deprived for 3 days and treated with 5 mM of KI and 5 mM of mannitol. Plants kept on the same renewed medium were used as control. Values are means ± s.e.m (n= 4).

Fig. 8. *hho* quadruple mutant displays ROS-related phenotypes following N treatment (A) Ascorbate Peroxidase (APX), glutathione peroxidase (GPX) and Glutathione Reductase activities (GR) of WT and *hho* quadruple mutant. Plants were grown for 4 weeks on hydroponic conditions +N (1 mM NH_4NO_3) then transferred to either +N (5 mM KNO_3) or –N (5 mM KCl mock control) for 3 days and finally treated with 5mM KNO_3 for 3 hours. **(B)** NBT staining of WT and quadruple *hho* mutant. Plants were grown on Petri dishes for 2 weeks on 0.5 mM NH_4NO_3. Fresh plants were harvested and directly stained with NBT. Leaves of the mutant plants display strong decrease in NBT coloration reporting a defect in superoxide accumulation. **(C)** ROS signature genes are controlled by NO_3^- and by HRS1 nuclear entrance. ROS signature genes (Vaahtera et al., 2014) were clustered on HRS1 TARGET data (Fig. 5b). ROS signature genes were color-coded according to their responsiveness to different sorts of ROS (red: hydrogen peroxide, blue: singlet oxygen, purple: superoxide, cyan: ozone) and according to statistical analysis. ANOVA followed by a Tukey test were performed. If a gene was significantly regulated (pval < 0.05) based on an ANOVA or a Tukey factor (Nitrate, DEX, Nitrate x DEX or a difference in the Tukey analysis (+/- DEX in +N or –N context)) a black square is reported in the clustering.

Fig. 9. Proposed model of the regulation of NSR by HHOs and ROS. On –N conditions, ROS are produced and are needed for the NSR induction. When Nitrogen is present in the media, HRS1 and its homologs are rapidly and highly expressed to repress NSR either directly by regulating *NRT2* and *GDH3* promoter activities or indirectly by reducing ROS production.

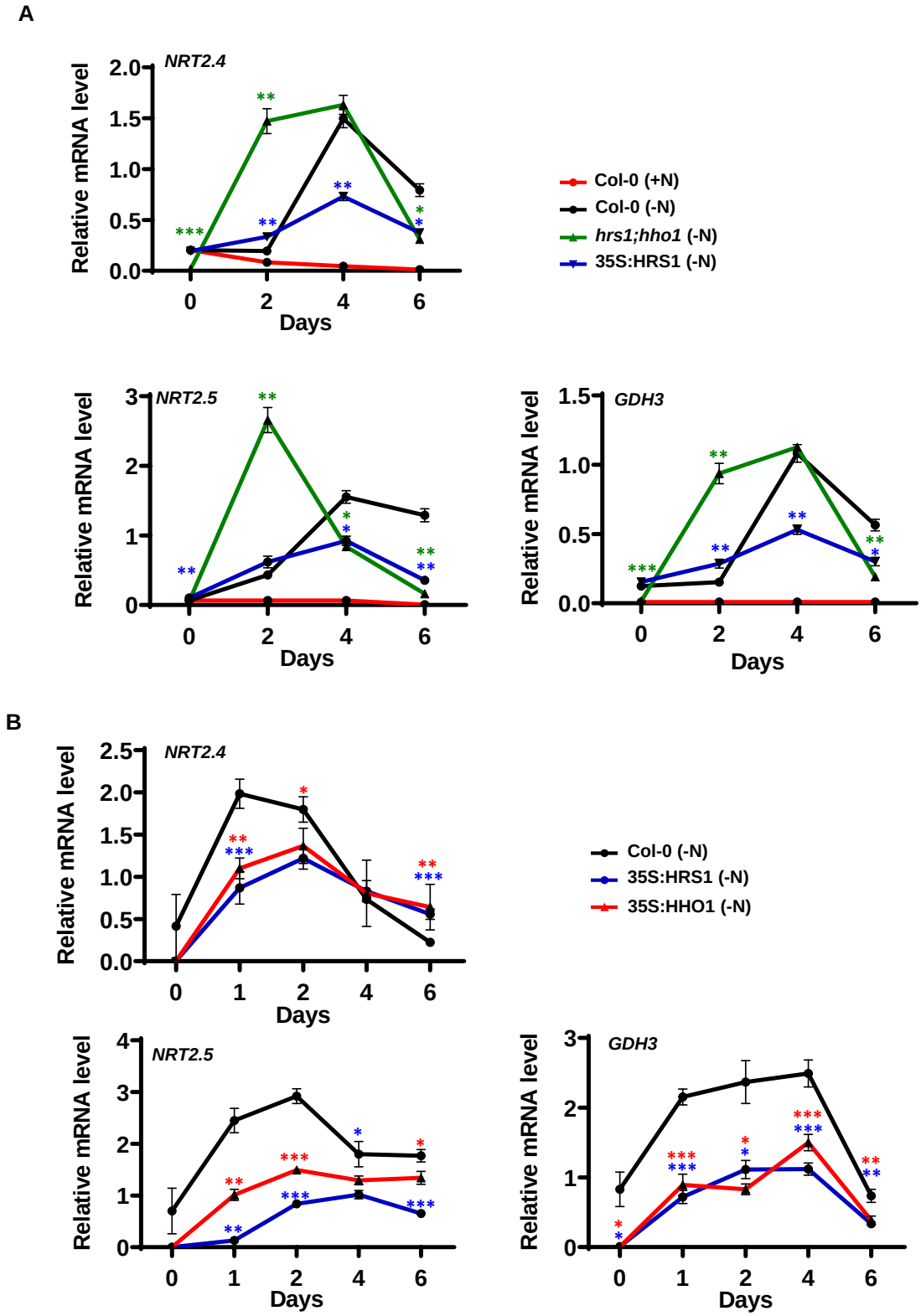

Fig. 1. HRS1 and HHO1 are repressors of NSR sentinel genes. (A) Root response of *NRT2.4*, *NRT2.5* and *GDH3* to NSR in Columbia, *hrs1;hho1*, 35S:HRS1 genotypes. Plants were grown in sterile hydroponic conditions on N-containing medium for 14 days. At time 0, the medium was shifted to –N conditions for 0, 2, 4, 6 days or +N as a control. **(B)** Root response of *NRT2.4*, *NRT2.5* and *GDH3* to NSR in Columbia WT, 35S:HRS1, 35S:HHO1 genotypes. Plants were grown in sterile hydroponic conditions on N-containing medium for 14 days. Then the medium was shifted to –N conditions for 0, 1, 2, 4, 6 days (the media background was kept unchanged). All transcript levels were quantified by qPCR and normalized to two housekeeping genes (*ACT* and *CLA*), values are means ± s.e.m (n= 4). Asterisks indicate significant differences from WT plants (*P<0.05; **P<0.01; ***P<0.001; Student's t-test).

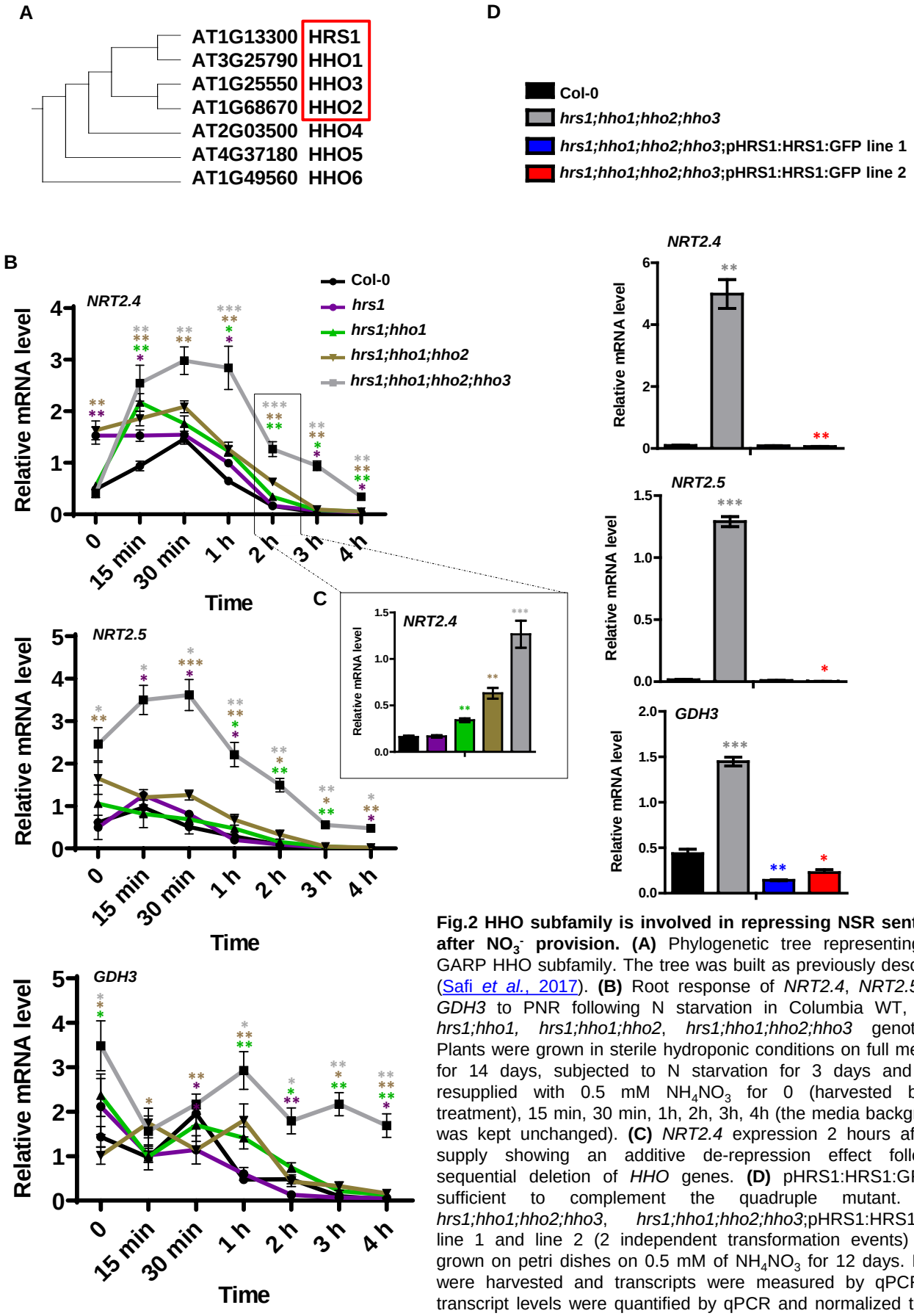

Fig.2 HHO subfamily is involved in repressing NSR sentinels after NO_3^- provision. (A) Phylogenetic tree representing the GARP HHO subfamily. The tree was built as previously described (Safi *et al.*, 2017). **(B)** Root response of *NRT2.4*, *NRT2.5* and *GDH3* to PNR following N starvation in Columbia WT, *hrs1*, *hrs1;hho1*, *hrs1;hho1;hho2*, *hrs1;hho1;hho2;hho3* genotypes. Plants were grown in sterile hydroponic conditions on full medium for 14 days, subjected to N starvation for 3 days and then resupplied with 0.5 mM NH_4NO_3 for 0 (harvested before treatment), 15 min, 30 min, 1h, 2h, 3h, 4h (the media background was kept unchanged). **(C)** *NRT2.4* expression 2 hours after N supply showing an additive de-repression effect following sequential deletion of *HHO* genes. **(D)** pHRS1:HRS1:GFP is sufficient to complement the quadruple mutant. WT, *hrs1;hho1;hho2;hho3*, *hrs1;hho1;hho2;hho3*;pHRS1:HRS1:GFP line 1 and line 2 (2 independent transformation events) were grown on petri dishes on 0.5 mM of NH_4NO_3 for 12 days. Roots were harvested and transcripts were measured by qPCR. All transcript levels were quantified by qPCR and normalized to two housekeeping genes (*ACT* and *CLA*), values are means ± s.e.m (n= 4). Asterisks indicate significant differences from WT plants (*P<0.05; **P<0.01; ***P<0.001; Student's t-test).

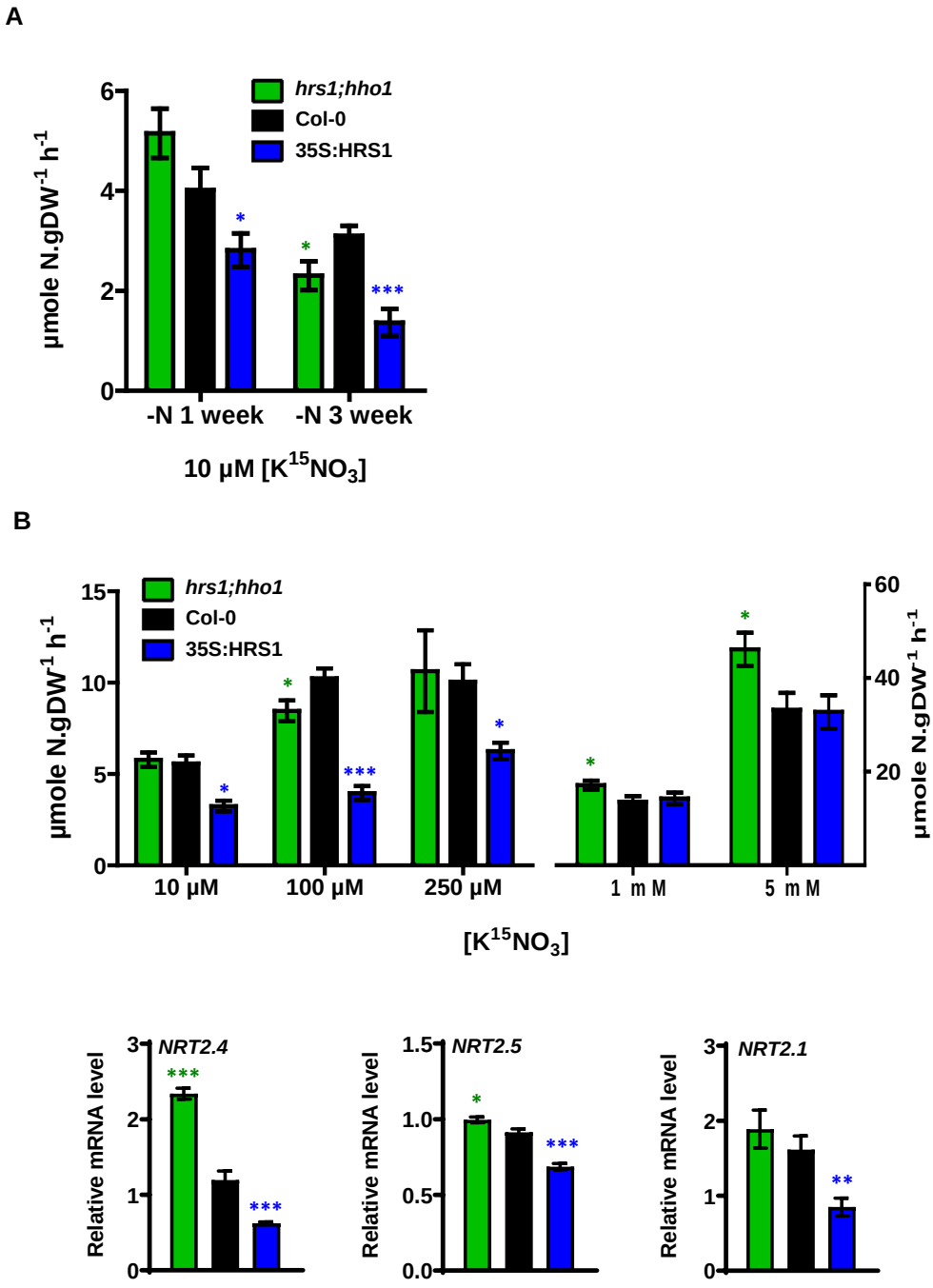

Fig. 3. HRS1 and HHO1 negatively control NO_3^- HATS. (A) NO_3^- uptake is altered in the 35S:HRS1 and in the double mutant *hrs1;hho1*. Plants were grown for 5 weeks on N-containing medium. The medium was then shifted to –N conditions or +N as a control for 1 or 3 weeks. Values are means ± s.e.m (n= 6). **(B)** One week-starved plants were used to quantify NO_3^- HATS and LATS activities as well as high affinity NO_3^- transporter transcript levels. qPCR data were normalized to two housekeeping genes (*ACT* and *CLA*), values are means ± s.e.m (n= 12). NO_3^- uptake measurements were performed on different $^{15}NO_3^-$ concentrations (10, 100, 250 µM, 1 and 5 mM) to evaluate HATS and LATS. Values are means ± s.e.m (n= 6). The experiment was performed exactly as mentioned for (a). Asterisks indicate significant differences from WT plants (*P<0.05; **P<0.01; ***P<0.001; Student's t-test).

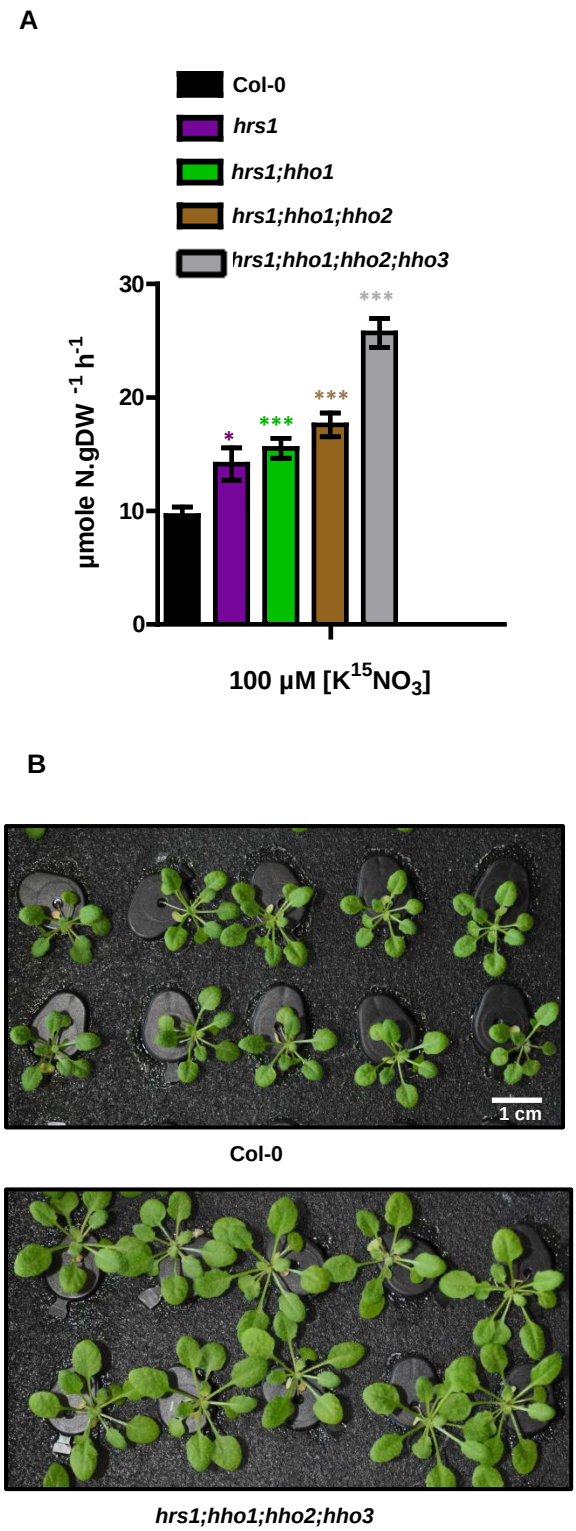

Fig. 4. The HHO subfamily represses NO_3^- uptake and growth in +N conditions.
(A) NO_3^- uptake is altered in *hrs1*, *hrs1;hho1*, *hrs1;hho1;hho2* and *hrs1;hho1;hho2;hho3* mutants. Plants were grown for 6 weeks on N-containing non-sterile hydroponics (0.5 mM NH_4NO_3). NO_3^- uptake measurements were performed at 100 µM $^{15}NO_3^-$ to evaluate the HATS. Values are means ± s.e.m (n= 6). Asterisks indicate significant differences from WT plants (*P<0.05; **P<0.01; ***P<0.001; Student's t-test). **(B)** Representative pictures of WT and *hrs1;hho1;hho2;hho3* quadruple mutant, grown on +N conditions, at the day of the uptake experiment show a growth phenotype.

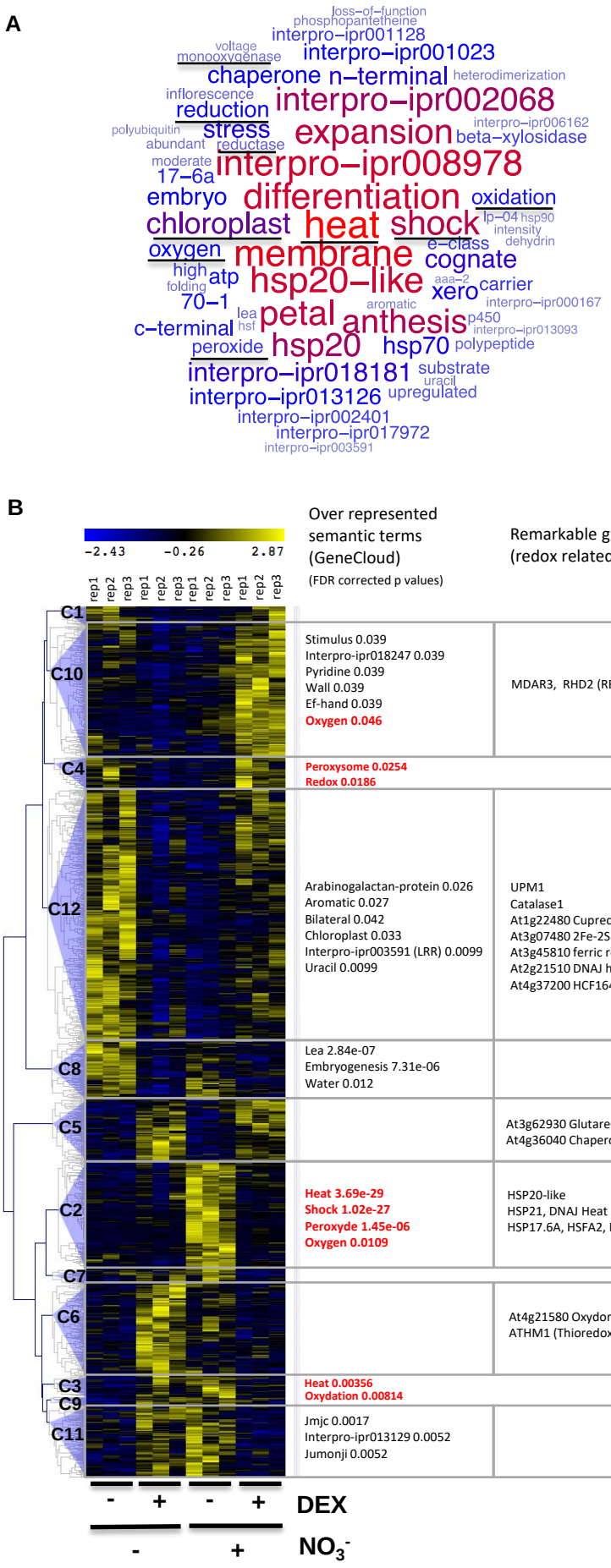

Fig. 5. HRS1 direct genome-wide targets are largely NO_3^--dependent and contain many redox-related genes. TARGET procedure was performed with NO_3^- (data from (Medici *et al.*, 2015)) and without NO_3^- (this work). An ANOVA analysis followed by a Tukey test retrieved 1050 HRS1-regulated genes (ANOVA pval cutoff 0.01, Tukey pval cutoff 0.01, FDR<10%). **(A)** GeneCloud analysis (Krouk *et al.*, 2015) of the 1050 direct targets of HRS1. **(B)** Clustering analysis (Pearson correlation) was performed using MeV software (number of clusters was determined by the FOM method). A selection of over-represented semantic terms is displayed in front of each cluster. Notable redox-related genes are displayed in the right column. The list of each cluster, their related gene list, as well as their respective semantic analysis are provided in Dataset S1.

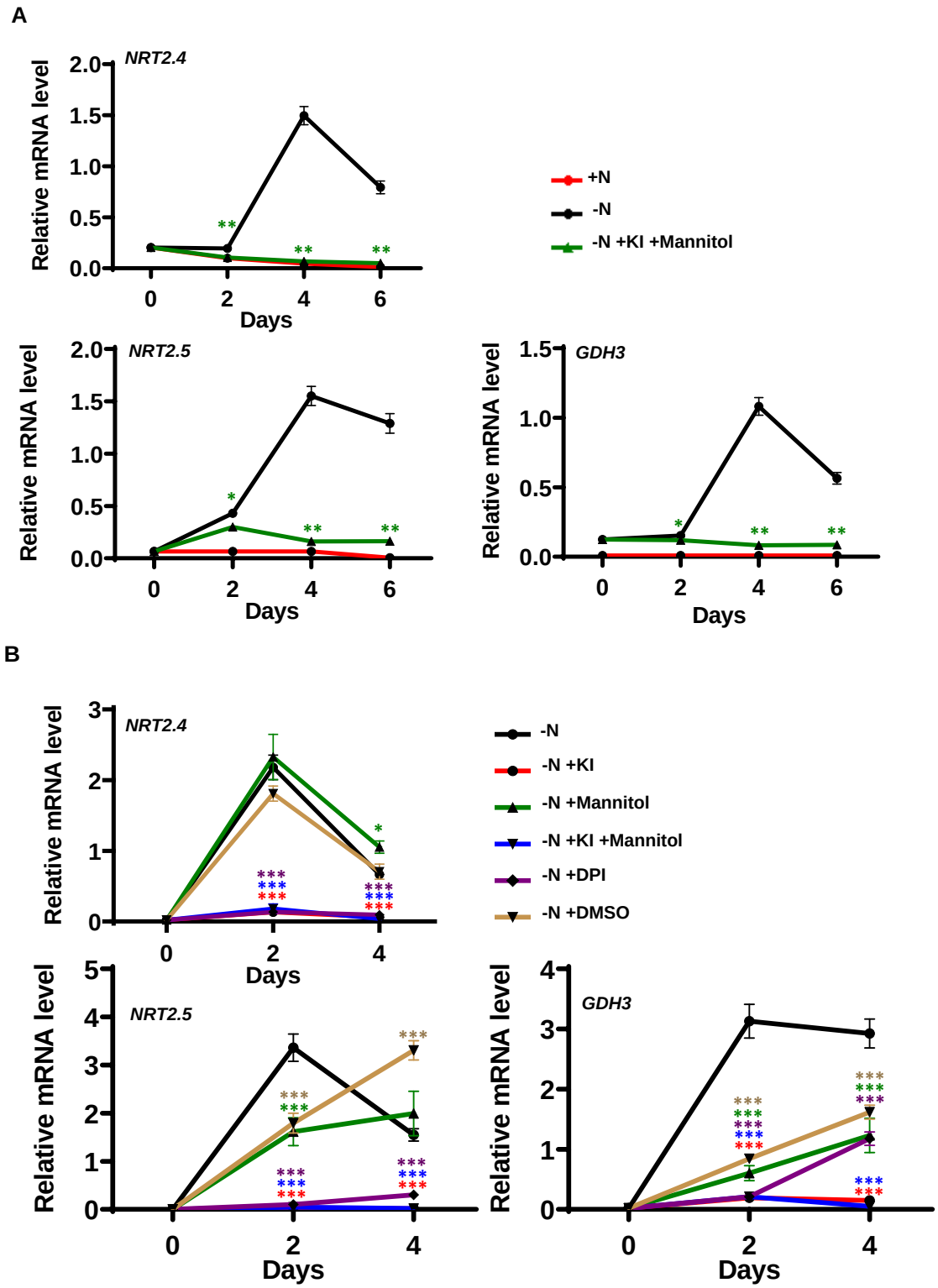

Fig. 6. ROS are necessary for NSR. (A) Altered response of *NRT2.4*, *NRT2.5* and *GDH3* by KI-mannitol treatment. Plants were grown in sterile hydroponic conditions on N-containing medium for 14 days. Thereafter, the medium was shifted to –N conditions containing or not 5 mM of KI and 5 mM of mannitol for 0, 2, 4, 6 days or +N as a control. **(B)** Altered response of *NRT2.4*, *NRT2.5* and *GDH3* by ROS scavenger treatment. Plants were grown in sterile hydroponic conditions on N-containing medium for 14 days. Then they were transferred to –N or +N conditions for 0, 2, 4 days. In parallel, some of the N-starved plants were treated with 5 mM KI, 5 mM mannitol, combination of both or with 10 µM DPI. DMSO was used as a mock treatment of DPI. All transcript levels were quantified by qPCR and normalized to two housekeeping genes (*ACT* and *CLA*), values are means ± s.e.m (n= 4). Asterisks indicate significant differences from WT plants (*P<0.05; **P<0.01; ***P<0.001; Student's t-test).

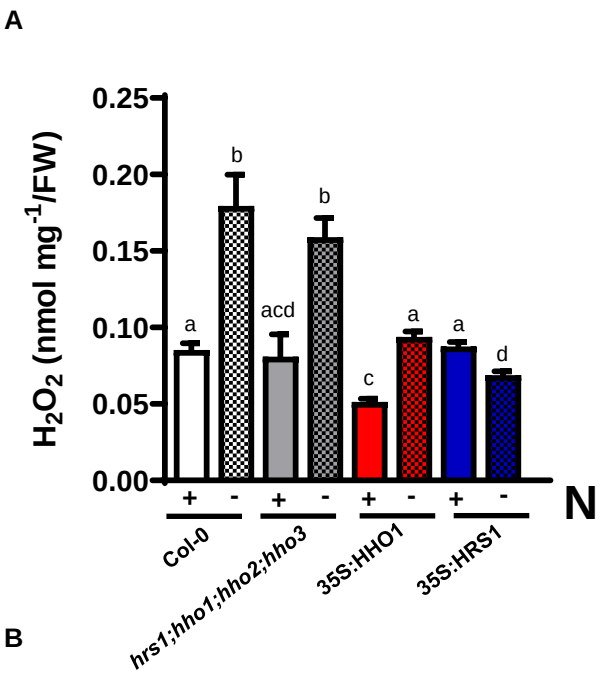

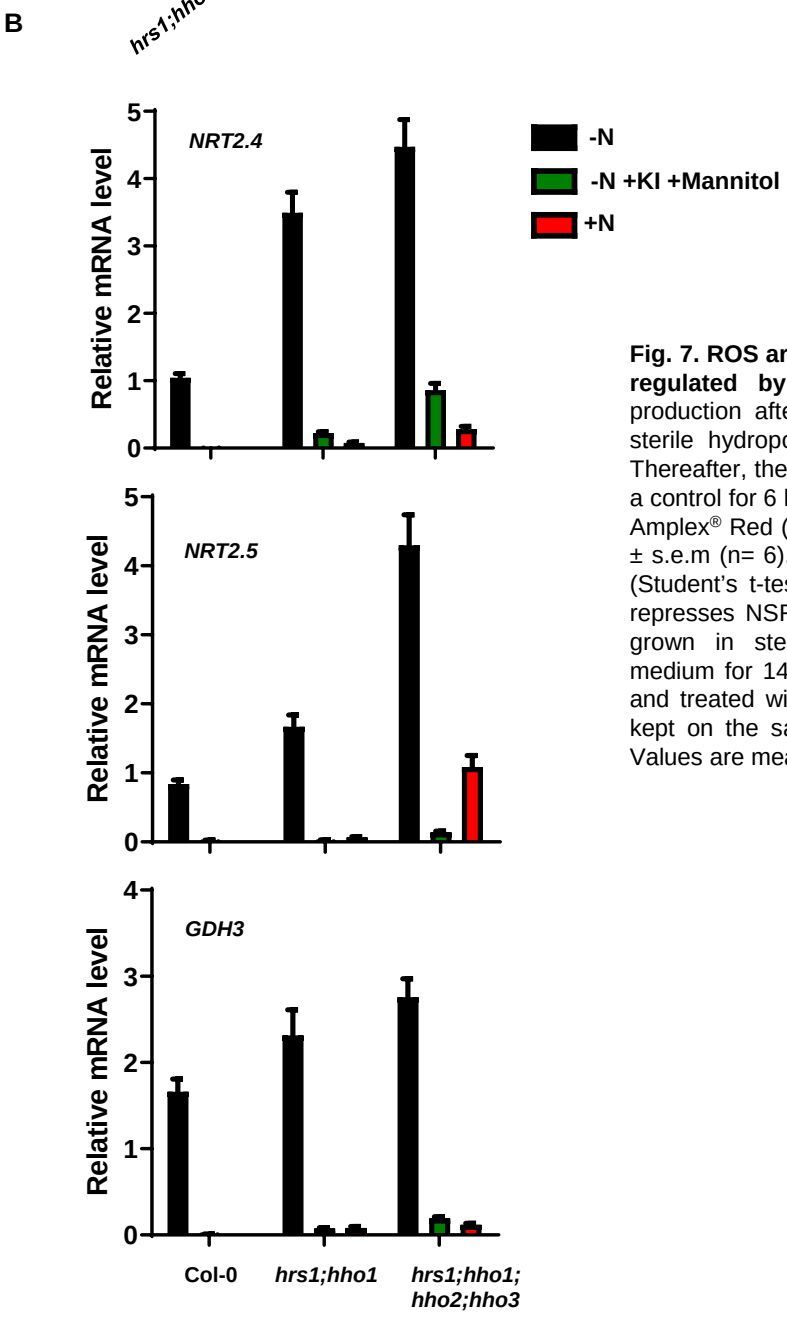

Fig. 7. ROS are produced early after nitrogen deprivation, regulated by HRS1 and crucial for NSR. (A) H_2O_2 production after N deprivation. Plants were grown in non-sterile hydroponics for 6 weeks on N-containing medium. Thereafter, the medium was shifted to –N conditions or +N as a control for 6 hours. H_2O_2 accumulation was measured using Amplex® Red (see Material and Methods). Values are means ± s.e.m (n= 6). Different letters means significant differences (Student's t-test, $P < 0.05$). **(B)** ROS-scavenging treatment represses NSR sentinel genes in *hho* mutants. Plants were grown in sterile hydroponic conditions on N-containing medium for 14 days. They were then N-deprived for 3 days and treated with 5 mM of KI and 5 mM of mannitol. Plants kept on the same renewed medium were used as control. Values are means ± s.e.m (n= 4).

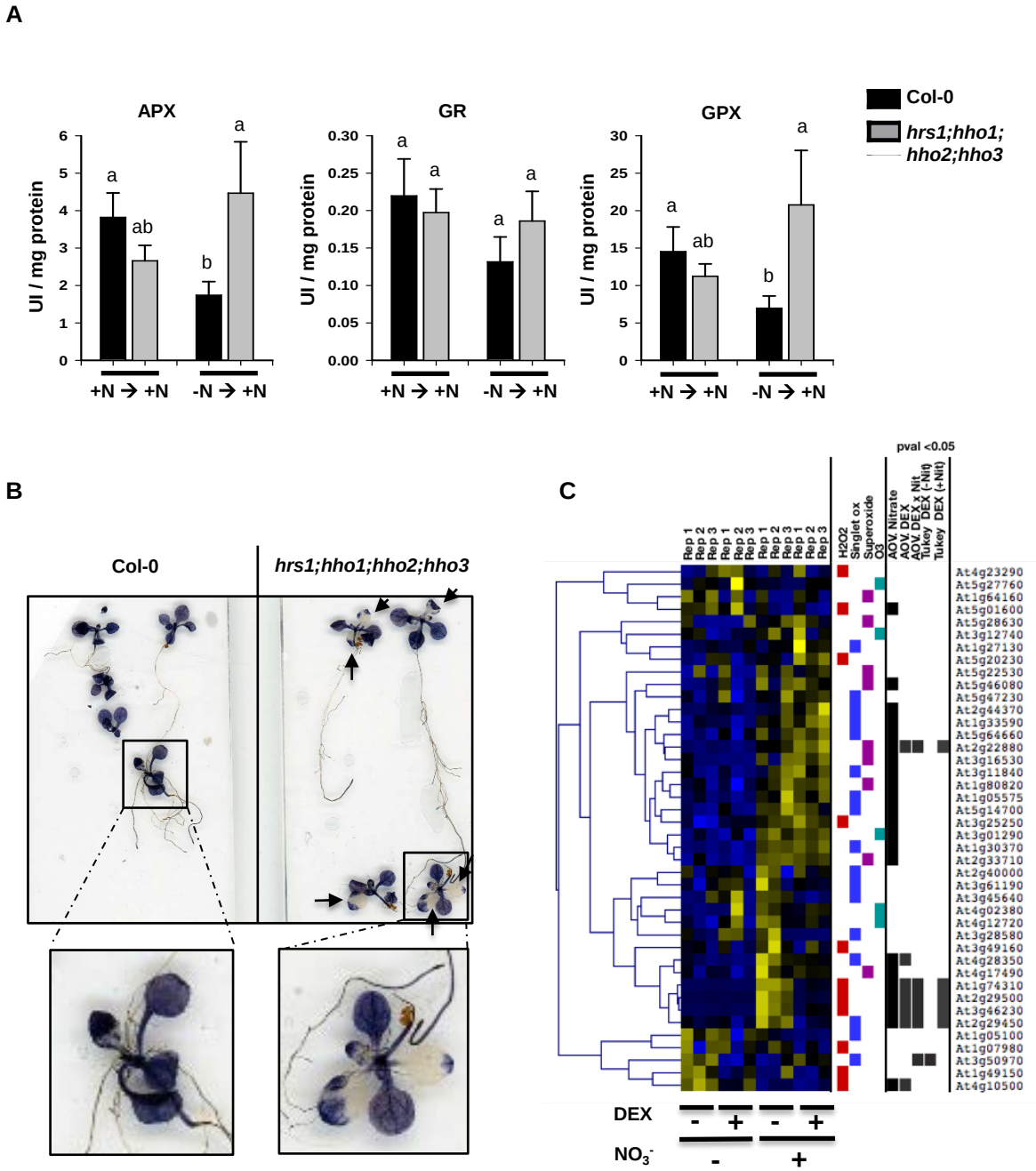

Fig. 8. *hho* quadruple mutant displays ROS-related phenotypes following N treatment (A) Ascorbate Peroxidase (APX), glutathione peroxidase (GPX) and Glutathione Reductase activities (GR) of WT and *hho* quadruple mutant. Plants were grown for 4 weeks on hydroponic conditions +N (1 mM NH_4NO_3) then transferred to either +N (5 mM KNO_3) or –N (5 mM KCl mock control) for 3 days and finally treated with 5mM KNO_3 for 3 hours. **(B)** NBT staining of WT and quadruple *hho* mutant. Plants were grown on Petri dishes for 2 weeks on 0.5 mM NH_4NO_3. Fresh plants were harvested and directly stained with NBT. Leaves of the mutant plants display strong decrease in NBT coloration reporting a defect in superoxide accumulation. **(C)** ROS signature genes are controlled by NO_3^- and by HRS1 nuclear entrance. ROS signature genes (Vaahtera *et al.*, 2014) were clustered on HRS1 TARGET data (Fig. 5b). ROS signature genes were color-coded according to their responsiveness to different sorts of ROS (red: hydrogen peroxide, blue: singlet oxygen, purple: superoxide, cyan: ozone) and according to statistical analysis. ANOVA followed by a Tukey test were performed. If a gene was significantly regulated (pval < 0.05) based on an ANOVA or a Tukey factor (Nitrate, DEX, Nitrate x DEX or a difference in the Tukey analysis (+/- DEX in +N or –N context)) a black square is reported in the clustering.

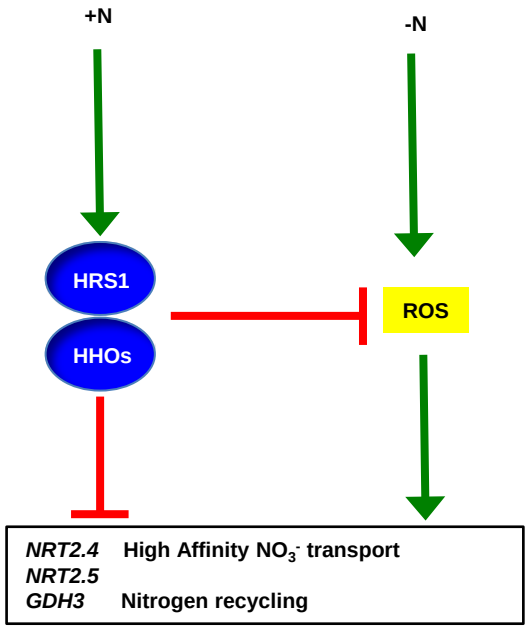

Fig. 9. Proposed model of the regulation of NSR by HHOs and ROS. On –N conditions, ROS are produced and are needed for the NSR induction. When Nitrogen is present in the media, HRS1 and its homologs are rapidly and highly expressed to repress NSR either directly by regulating *NRT2* and *GDH3* promoter activities or indirectly by reducing ROS production.